Naval Research Laboratory

Washington, DC 20375-5000

NRL Memorandum Report 6784

Background Simulation and Filter Design Using Iterated Function Systems

IRA B. SCHWARTZ

Plasma Physics Division
Special Project in Nonlinear Science

LAURIE REUTER

George Washington University
Dept. of EE and CS
Washington, DC

and

Bellcore, MRE 2M-344, 445 South St.,
Morriston, NJ 07960-1910

February 19, 1991

REPORT DOCUMENTATION PAGE

Form Approved
OMB No 0704-0188

1. AGENCY USE ONLY (Leave blank)	2. REPORT DATE	3. REPORT TYPE AND DATES COVERED
	1991 February 19	Interim

4. TITLE AND SUBTITLE

Background Simulation and Filter Design Using Iterated Function Systems

5. FUNDING NUMBERS

47-3638-01

6. AUTHOR(S)

Ira B. Schwartz and Laurie Reuter*

7. PERFORMING ORGANIZATION NAME(S) AND ADDRESS(ES)

Naval Research Laboratory
Code 4700.3
Washington, DC 20375-5000

8. PERFORMING ORGANIZATION REPORT NUMBER

NRL Memorandum Report 6784

9. SPONSORING/MONITORING AGENCY NAME(S) AND ADDRESS(ES)

Office of Naval Research
Arlington, VA 22203

10. SPONSORING/MONITORING AGENCY REPORT NUMBER

RR 014-0241

11. SUPPLEMENTARY NOTES

*George Washington University, Dept. of EE and CS, Washington, DC
Bellcore, MRE 2M-344, 445 South St., Morriston, NJ 07960-1910

12a. DISTRIBUTION/AVAILABILITY STATEMENT

Approved for public release; distribution unlimited.

12b. DISTRIBUTION CODE

13. ABSTRACT *(Maximum 200 words)*

Design of filters which detect known signals in unknown backgrounds are considered from a deterministic viewpoint. Backgrounds which appear in Nature rather than being smooth, may appear fractal within a given waveband of interest. In this paper, derivations are given for the design of filters for both smooth backgrounds, and fractal backgrounds. The main theoretical tool for the fractal design is the Iterated Function System (IFS). It is shown how the IFS models generalize the smooth models of the background and the corresponding filters. Derivations of the false alarm rate in terms of the filters are given. Numerical examples demonstrating background simulation as well as convolution of the filters with signals embedded in noise having fractal dimension are presented.

14. SUBJECT TERMS

Fractals
Iterated Functions Systems
Filters
Nonlinear dynamics

15. NUMBER OF PAGES

52

16. PRICE CODE

17. SECURITY CLASSIFICATION OF REPORT	18. SECURITY CLASSIFICATION OF THIS PAGE	19. SECURITY CLASSIFICATION OF ABSTRACT	20. LIMITATION OF ABSTRACT
UNCLASSIFIED	UNCLASSIFIED	UNCLASSIFIED	SAR

CONTENTS

BACKGROUND SIMULATION AND FILTER DESIGN USING ITERATED FUNCTION SYSTEMS

0 Introduction:

One of the basic problems in signal processing is that of determining whether a known signal embedded in a noisy environment can be detected using some sort of algorithm. Typically, the signal is perturbed by an unknown noise source, and the algorithm is a convolution of a filter with a signal. (For a review of linear filtering theory, see Kalaith,1974.) The convolution may be adaptive over the signal [Stein,1987], or it may be fixed, as in the matched filter [Gardner, 1986, pp.269-272]. In the case of the matched filter, the filtered signal-to-noise ratio is maximized by enhancing those frequencies that are above the noise power, and de-emphasizing those frequencies for which the signal is noise dominated. Typically, matched filters fall into one of three well- known types: low pass filters, high pass filters, and (mid-)band pass filters. The design of such a filter requires that the statistics of the noise be known apriori. In particular, the autocorrelation (equivalently, the power spectrum [van Kampen,1981,p.62]) must be known. As a result, almost all filters that are applied to wide sense stationary processes having a known power spectrum are designed in the frequency domain by using Fourier transforms.

On the other hand, Nature exhibits examples in which the statistics of the noise are unknown in space and/or time, or the statistics may be non-stationary. In this case, a matched filter for a known signal cannot be designed, since the power spectrum is unknown. Alternatively, in addition to being unknown, the spectrum may be spread over a large range of frequencies. Examples of noise possessing such a range are 1/f noise [West,1989], or broadband noise of a chaotic attractor [Parker,1987]. The implication is that it may not be advantageous to design a filter in the frequency domain, but instead work in the space-time domain. We define a filter designed using a least mean squares technique to be a least mean squares filter (LMSF).

The goals of this paper are twofold. First, we derive a three-dimensional filter designed in a space-time domain to detect a known signal in an unknown but smooth background. We assume the background to be smooth in order to demonstrate the technique of filter design and background modelling. In the detection of moving objects or the extraction of moving features from a bank of images, the three dimensional domain consists of two space dimensions and one time dimension. We remark here that the modeling of smooth backgrounds deterministically has also been considered in [Chen,1989] and [Longmire et al, 1988] in feature extraction problems.

Although models for, and filters based upon smooth backgrounds are easy to derive, they are crude approximations when trying to model backgrounds which are nonsmooth. Examples of nonsmooth backgrounds abound in nature in which there is no preferred length scale over a particular wave band. Such nonsmooth examples occur as fractal cloud boundaries [Lovejoy,1982,1985,1986], fractal properties of wind driven sea states [Barenblatt,1981;Elgar,1989;Stiassne,1986;, and Zaslavskii, 1987], and 1/f noise [West,1989].

Manuscript approved November 7, 1990.

The prototypical example of a nonsmooth curve is the well-known Weierstrass function, which is continuous everywhere, but nowhere differentiable . Hughs [1980] demonstrates that the Weirstrass function is fractal. Another example of a nonsmooth curve generated by a stochastic process is Brownian motion [Wong, 1985,pp. 46ff]. It too can be shown, in a probabilistic sense, to be fractal. Therefore, our second goal is to model deterministically a nonsmooth but continuous background, such as the Weierstrass function, in one-dimension.

Since the backgrounds we are dealing with are fractal, the tools of choice used in modelling them used are those of Iterated Function Systems (IFS) [Barnsley, 1988]. Current and past research in IFS theory has focused on data compression, and not filter design. The main result of this paper is the design of a linear filter which models (in a least squares sense) a fractal background and detects a known signal shape. Furthermore, the unknown background may be simulated as an attractor of a nonlinear dynamical system which consists of a set of a small number of chosen maps, yielding information about the roughness or dimension of the background. The advantage of using such an approach is that self similar backgrounds having fractal dimensions, such as cloud edges and cloud intensities, may be modelled with only a few parameters.

The layout of the paper is as follows. Section 1 contains the design of a three dimensional linear filter for a smooth background. The analysis of the filter on known smooth backgrounds is done in Section 2. When the background is assumed to be a correlated Gaussian, a multivariate statistical formulation of the filter along with its performance is given in Section 3. In many applications, it is useful to know how the LMSF performs with a background that is normal. If the background noise is Gaussian and uncorrelated, then a matched-filter detector minimizes the probability of detection error when a threshold is properly set and applied to the filtered signal [van trees, 1968, pp.286-290]. One relevant criterion used in characterizing the probability of error detection is the probability of detection of a signal that is not present, called a probability of false alarm (PFA). It is shown in this paper how the PFA depends upon the LMS filter weights. Section 4 briefly describes the machinery of an iterated function system (IFS), and the basic results needed to simulate a known background. Section 5 extends the analysis to the design of a model of an unknown background in terms of an IFS. Numerical examples of the IFS-based filter are given in Section 6. Our conclusions are presented in section 7.

1.0 Three dimensional filter design on smooth backgrounds:

This section sets up the notation and machinery to detect a known time-dependent signal moving through space. The signal may have a time-dependent intensity or brightness. Examples of a known signal would be an aircraft having a given velocity moving across a sensor's field-of-view, a moving boundary in an experiment, or a communications signal

in the presence of noise. The noise or clutter might be the brightness from a bank of clouds, sensor noise, turbulence, or low dimensional noise such as noise generated deterministically that is chaotic. Much work has been done in feature extraction, or the detection of features in one and two dimensions [See Chen,1989, for example] for smooth backgrounds, but we begin with the analysis of a three dimensional space. The main advantages of incorporating time is an overall increase in performance of the receiver operating characteristics [Scribner, et al, 1988].

To formulate the problem, define the spatio-temporal location of the signal by coordinates $x_i = (x^1_i, x^2_i, x^3_i)$. The signal maps out a smooth curve C as a function of time t,

$$C: \begin{bmatrix} x^1 \\ x^2 \\ x^3 \end{bmatrix} = \begin{bmatrix} \gamma_1(t) \\ \gamma_2(t) \\ \gamma_3(t) \end{bmatrix}, t \in [t_0, t_1]. \tag{1.1}$$

where γ_i, i=1,2,3 are smooth functions. We will think of the problem as being analyzed in a stack of image planes, with each discrete coordinate in each plane denoting a pixel. The coordinates are discretized at times t_i; i.e., $(x^1_i, x^2_i, x^3_i) = (\gamma_1(t_i), \gamma_2(t_i), \gamma_3(t_i))$ is the location of the i^{th} pixel. Following Pratt [1978, page 127], pixels are ordered by columns, as illustrated in the example below.

Example of column ordering:

$$\begin{bmatrix} 1 & | & 3 \\ X & | & \\ - & - & - \\ 2 & | & 4 \end{bmatrix} \qquad \begin{bmatrix} 5 & | & 7 \\ & | & X \\ - & - & - \\ 6 & | & 8 \end{bmatrix}. \tag{1.2}$$

$$x^3 = 1 \qquad x^3 = 2$$

In the example, there are two 4X4 frames of data at times x^3=1 and x^3=2. If the signal appears in the pixels labelled 1 and 7 in the above two frames, then we assign signal coordinate (1,1,1) to pixel 1 and (1,2,2) to pixel 7.

Now suppose the signal brightness at pixel i is a function of position (x^1, x^2, x^3), i.e.,

$$s_i = \hat{s}(x_i), \tag{1.3}$$

where $\hat{s}$ is a scalar function of $\mathbf{x}_i = (x^1_i, x^2_i, x^3_i)$. Since the signal is a function of 3 dimensions, the filter designed will be a 3D filter. (For other examples of 3-D filtering, see Reed et al, 1988, Hecht-Nielsen,1987.)

If $N_{x1}, N_{x2}, and\ N_{x3}$ denote the number of pixels in the 3 directions, the total number of pixels that needs to be considered is $K = N_{x1} \cdot N_{x2} \cdot N_{x3}$. Each pixel has some probability of containing a time dependent signal and background. Designing a filter based upon an unknown background that is smoothly varying in both space and time requires that the background be approximated by some model. Suppose the signal and background are added together. The model of the signal at pixel i consists of a triple designating space and time coordinates given by x_i, and a brightness given by s_i. (Here i ranges over the number of pixels K.) Assume the center-of-mass of the 3-D grid is the origin, and $x^1_i \varepsilon \left[\frac{-N_{x^1}}{2}, \frac{N_{x^1}}{2}\right]$, $x^2_i \varepsilon \left[\frac{-N_{x^2}}{2}, \frac{N_{x^2}}{2}\right]$ and $x^3_i \varepsilon \left[\frac{-N_{x^3}}{2}, \frac{N_{x^3}}{2}\right]$. Since the approximation of the background is assumed to be smooth in space and time, the background can be modeled locally at each pixel by a Taylor series expansion in $\mathbf{x}$ about the origin. Specifically, the i^{th} component of the model is given by

$$[\hat{f}(x, s)]_i = A_1 \cdot s_i + A_2 \cdot u_i + B_{1j} \cdot x^j_i + B_{2jk} \cdot x^j_i \cdot x^k_i + B_{3jkl} \cdot x^j_i \cdot x^k_i \cdot x^l_i + \ldots \tag{1.4}$$

where $\hat{f}$ is a K-dimensional vector function of $\mathbf{x} = (\mathbf{x_1}, \mathbf{x_2}, \ldots, \mathbf{x_K})$ and $\mathbf{s} = (s_1, s_2, \ldots, s_K)$. In Eq. (1.3) i runs from 1 to K and repeated superscripts j,k,l are assumed to be summed over their limits. The j^{th} component of the vector $\mathbf{u}$ is defined by $[\mathbf{u}]_j = 1$, $j = 1,\ldots,K$, and denotes the constant level of the background, implying it is not necessary that the background have zero mean. The first term on the RHS of Eq. (1.3) is proportional to the signal strength at (x^1_i, x^2_i, x^3_i). The remaining terms model linear and higher order variations in the background. The coefficients $A_1, A_2, B_{1j}, \ldots$, are constants to be determined. Notice that for each polynomial of degree m in the background approximation, there are at most $\binom{3+m-1}{m} = \frac{(3+m-1)!}{m!2!}$ distinct monomials of degree m. Less than this number can be allowed since some directions may not be as smooth as others. For example, in some cases it may be sufficient to assume that the background is linear in time and quadratic in space.

The above notation is compressed in the following way. Introduce the K-dimensional vectors $\mathbf{z}_j$, where the i^{th} component is defined by

$$[z_1]_i = s_i \qquad [z_2]_i = u_i \qquad [z_3]_i = x_i^1 \qquad [z_4]_i = x_i^2$$

$$[z_5]_i = x_i^3 \qquad [z_6]_i = x_i^1 \cdot x_i^1 \; [z_7]_i = x_i^1 \cdot x_i^2 \qquad [z_8]_i = x_i^1 \cdot x_i^3$$

$$[z_9]_i = x_i^2 \cdot x_i^2 \quad [z_{10}]_i = x_i^2 \cdot x_i^3 \qquad [z_{11}]_i = x_i^3 \cdot x_i^3 \cdot \ldots \tag{1.5}$$

Using this transformation, the model in Eq. (1.4) may be written in the simplified form

$$f(A) = \sum_{i=1}^{M+2} A_i \cdot z_i, \tag{1.6}$$

where **f** is a function mapping R^{M+2} to R^K. The value of M is the number of monomials having degree less than or equal to m; i.e.,

$$M = \sum_{j=1}^{m} \binom{3+j-1}{j}. \tag{1.7}$$

The vector of parameters, $\mathbf{A} = (A_1, \ldots, A_{M+2})$, is to be determined.

Letting the K measured observations at each pixel be denoted by the vector v, define the residual error to be $\mathbf{e(A) = f(A) - v}$. The residual error is to be minimized by finding **A** such that $\|e\|^2$ is minimized in the Euclidean norm. Minimization of the residual error results in a least squares problem, and is equivalent to finding an M+2 dimensional vector **A** that satisfies the normal equations

$$\left.\frac{\partial f^t}{\partial A}\right|_A \bullet (f(A) - v) = 0 \tag{1.8}$$

Since **f** is a linear function of **A**, the matrix of coefficients is independent of **A**., and Eq. (1.8) may be written as

$$S \cdot A = \left.\frac{\partial}{\partial A} f\right|_A \cdot v \tag{1.9}$$

where **S** is a symmetric matrix having its ij^{th} element given by $z_i^t \cdot z_j$.

Now suppose **S** is nonsingular, and let **B** be its inverse. Then Eq. (1.8) can be solved for **A** uniquely. In particular, since

$$\left[\frac{\partial}{\partial A} f\right]_A \cdot v\Big]_j = z_j^t \cdot v, \tag{1.10}$$

the signal coefficient A_1 is given by

$$A_1 = \sum_{j=1}^{M+2} [B]_{1j} \cdot z_j^t v \tag{1.11}$$

$$= \sum_{k=1}^{K} \left(\sum_{j=1}^{M+2} [B]_{1j} \cdot [z_j]_k \right) [v]_k \tag{1.12}$$

Coefficient A_1 now may be written as a one dimensional convolution. Let w be a K-dimensional vector with k^{th} component defined by

$$[w]_{K+1-k} = \sum_{j=1}^{M+2} [B]_{1j} [z_j]_k. \tag{1.13}$$

Then Eq.(1.11) may be written as

$$A_1 = \sum_{k=1}^{K} [w]_{K-k+1} [v]_k$$

$$= w^* v \tag{1.14}$$

The symbol * in Eq. (1.14) denotes a one dimensional convolution between the vectors w and v. Components of the vector w are the weights of a filter designed for a given signal s. The idea is that convolving w with any background that is smooth up to degree m in space and time should have a null result. This is indeed the case as will be shown in the next section.

2.0 Analysis of a three dimensional LMSF:

Suppose the vector v contains no signal, but has a smooth background (or clutter) given by

$$v = \sum_{j=2}^{M+2} C_j z_j \tag{2.1}$$

where the C_j are arbitrary real numbers and the z_j are defined in Section 1.

Proposition 2.1: For the background given in Eq. (2.1), if S is nonsingular, then $A_1 = 0$, and $A_i = C_i$, i=2,...,M+2

Proof: Using the background specified by Eq. (2.1) in the linear system of Eq. (1.9) results in solving a system of the form

$$S \cdot A = \Delta \cdot C \tag{2.2}$$

where Δ is an M+2 x M+1 matrix and C is vector whose components are $(C_2, C_3, ..., C_{M+2})$. The ijth component of Δ is given by $z_i^t z_j$, which implies that Δ is a minor of S.

Let $C_1 = 0$, and augment the right hand side of Eq. (2.2) as follows:

$$\left[\begin{array}{c|c} z_1^t z_1 & \\ \bullet & \\ \bullet & \Delta \\ \bullet & \\ z_{M+2}^t z_1 & \end{array}\right] = S \cdot \left[\begin{array}{c} C_1 \\ \hline C_2 \\ \bullet \\ \bullet \\ \bullet \\ C_{M+2} \end{array}\right]. \tag{2.3}$$

The result immediately follows from the nonsingularity of S.

If one used the filter weights derived in Section 1 and convolved the weights with the smooth background, a similar result holds.

*Proposition 2.2: Suppose v is as defined by Eq. (2.1). Then w * v = 0, where the components of w are given by Eq. (1.8).*

Proof: The result can be proven by direct computation. By using the linearity and definition of the convolution, we have

$$A_1 = \sum_{i=2}^{M+2} C_i \{ \sum_{k=1}^{K} [w]_{K+1-k} [z_i]_k \} . \tag{2.4}$$

Substituting the explicit expression for the components of the weight vector and simplifying yields

$$A_1 = \sum_{i=2}^{M+2} C_i \{ \sum_{j=1}^{M+2} [B]_{1j} z_j^t z_i \} . \tag{2.5}$$

Since $[S]_{ji} = z_j^t z_i$, and

$$\sum_{j=1}^{M+2} [B]_{1j} [S]_{ji} = 1, \text{ if i=1} \tag{2.6}$$

$$= 0, otherwise$$

the result follows because the outer summation on i in Eq. (2.5) does not include i = 1.

The two propositions show that the convolution of a smooth background up to terms of order specified by the model with the weight vector yields a signal amplitude that is zero. A given sequence of images, then, having this background, can always be considered to be zero after convolution.

3.0 Analysis of the filter on correlated Gaussian backgrounds

Multivariate Formulation: When formulated as a convolution, the LMS filter is generally thought of as operating on a smooth background. This section analyzes the operation of an LMS filter on a background that is normal with a given mean and covariance matrix.

In the previous section, it has been shown how the three dimensional background, filter and convolution are formulated in terms of one dimensional arrays. Specifically, if A_1 denotes the scalar result after convolving the filter with the background, it was shown that $A_1 = w*v$, which may be written as an inner product:

$$A_1 = \boldsymbol{a}^t \cdot \boldsymbol{v} \tag{3.1}$$

where $\mathbf{a},\mathbf{v} \in R^K$. If $\mathbf{w}$ is the vector whose components are the weights of the filter, then

$$a^t = (w_K, w_{K-1}, w_{K-2}, \ldots, w_1)$$

Suppose the vector v is a vector with each component a random variable (RV). In particular, v is assumed to be normal having mean μ and correlation matrix Σ. Let

$$n(v|\mu,\Sigma) = (2\pi)^{-\frac{1}{2}} \|\Sigma\|^{-\frac{1}{2}} exp\left(\left(-\frac{1}{2}\right)(v-\mu)^t \Sigma^{-1}(v-\mu)\right) \tag{3.2}$$

denote the multivariate normal density of RV v. The question addressed is, what effect do the weights have on the signal coefficient A_1? Specifically, what is the density of A_1? Since A_1 is a linear function of the RV v, it follows that the density of A_1 is also Normal. To see this, it is easy to construct a nonsingular transformation that maps v into another vector, say y, in R^n whose first component is A_1. Let the transformation be given by

$$y_1 = a^t v \tag{3.3}$$

$$y_i = v_i, \text{"i=2,K}$$

Therefore, there exists a matrix A such that y = Av, where det A = a_1 =0. The density corresponding to y is $n(y|A\mu, A\Sigma A^t)$). To get the marginal density for y_1 means integrating $y_2, y_3, \ldots, y_n$ from $-\infty$ to ∞. An alternative way to derive the density of A_1 is by partitioning the vector v. Let $V_1 = v_1 \in R^1$, and $V_2 \in R^{K-1}$, where $V_2^t = (v_2, \ldots, v_K)$. Thus

$$v = \begin{bmatrix} V_1 \\ V_2 \end{bmatrix}. \tag{3.4}$$

Likewise, the mean is partitioned as

$$\mu = \begin{bmatrix} \mu_1 \\ \mu_2 \end{bmatrix}. \tag{3.5}$$

The matrix Σ is partitioned into four submatrices by

$$\Sigma = \begin{bmatrix} \Sigma_{11} & \Sigma_{12} \\ \Sigma_{12}^t & \Sigma_{22} \end{bmatrix} \tag{3.6}$$

where

$$\begin{aligned}\Sigma_{11} &= E(V_1 - \mu_1)(V_1 - \mu_1)^t \\ \Sigma_{22} &= E(V_2 - \mu_2)(V_2 - \mu_2)^t \\ \Sigma_{12} &= E(V_1 - \mu_1)(V_2 - \mu_2)^t \\ \Sigma_{21} &= \Sigma_{12}^t\end{aligned} \tag{3.7}$$

The dimensions of Σ_{11}, Σ_{22}, Σ_{12} are (1 x 1), (K-1 x K-1), and (1 x K-1), respectively. In terms of the partitioned vectors, $A_1 = a_1 V_1 + a_2^t V_2$, where $a^t = (a_1, a_2^t)$.

Let y denote an n-dimensional vector, and partition y in a manner similar to v;i.e., $y^t = (Y_1, Y_2)$.

Proposition 3.1: If

$$\Sigma_{11} + a_2^t \cdot \Sigma_{21} \neq 0 \tag{3.8}$$

then there exists a nonsingular transformation $y = Tv$ *such that* $E(Y_1 - \nu_1)(Y_2 - \nu_2) \neq 0$, *where* $\nu_i = E(Y_i)$, $i = 1,2$.

The proposition implies that the RV's Y_1 and Y_2 are independent, even though V_1 and V_2 are not. Therefore the density of y is just the product of the Normal densities corresponding to Y_1 and Y_2.

Proof: Define the transformation by

$$\begin{aligned}Y_1 &= a_1 V_1 + a_2^t \cdot V_2 \\ Y_2 &= V_2 + b \cdot V_1\end{aligned} \tag{3.9}$$

where $b \epsilon R^{K-1}$. We claim there exists a b such that $0 = E(Y_1 - \nu_1)(Y_2 - \nu_2)^t$. Indeed,

$$\begin{aligned}0 &= E(Y_1 - \nu_1)(Y_2 - \nu_2)^t \\ &= E\{[a_1 V_1 + a_2^t \cdot V_2 - (a_1 \mu_1 + a_2^t \mu_2)] \bullet [V_2 + bV_1 - (\mu_2 + b\mu_1)]^t\} \\ &= a_1 \Sigma_{12} + a_2^t \cdot \Sigma_{22} + (\Sigma_{11} + a_2^t \cdot \Sigma_{21}) b^t\end{aligned} \tag{3.10}$$

Clearly, the cross-correlation is zero if and only if

$$b^t = \frac{(-a_1)\,\Sigma_{12} - (a_2^t \cdot \Sigma_{22})}{\Sigma_{11} + a_2^t \cdot \Sigma_{21}}. \tag{3.11}$$

The matrix of the transformation is given by

$$T = \begin{bmatrix} a_1 & a_2^t \\ b & I_{K-1} \end{bmatrix} \tag{3.12}$$

where I_{K-1} is the identity on R_{K-1}.

It is now a trivial matter to compute the diagonal correlation matrices. In particular,

$$\begin{aligned} \Psi_{11} &= E\,(Y_1 - \nu_1)\,(Y_1 - \nu_1) \\ &= a_1\Sigma_{11}a_1 + a_1\Sigma_{12}a_2 + a_2^t\Sigma_{12}^t a_1 + a_2^t\Sigma_{22}a_2 \\ &= a^t\Sigma a \end{aligned} \tag{3.13}$$

Likewise,

$$\begin{aligned} \Psi_{22} &= E\,(Y_2 - \nu_2)\,(Y_2 - \nu_2) \\ &= b\Sigma_{11}b^t + b\Sigma_{12} + [b\Sigma_{12}] + \Sigma_{22} \end{aligned} \tag{3.14}$$

Since $\Sigma_{12} = \Sigma_{21}^t = 0$, Y_1 and Y_2 are independently Normally distributed. If

$$\Psi = \begin{bmatrix} \Psi_{11} & 0 \\ 0 & \Psi_{22} \end{bmatrix} \tag{3.15}$$

then the exponent in the distribution is

$$\begin{aligned} Q &= (Y - \nu)^t \Psi^{-1} (Y - \nu) \\ &= (Y_1 - \nu_1)^t \Psi_{11}^{-1} (Y_1 - \nu_1) + (Y_2 - \nu_2)^t \Psi_{22}^{-1} (Y_2 - \nu_2) \end{aligned} \tag{3.16}$$

and the density for Y is given by

$$n\,(Y|\,\nu, \Psi) = n\,(Y_1|\,\nu_1, \Psi_{11})\,n\,(Y_2|\,\nu_2, \Psi_2) \tag{3.17}$$

By integrating over Y_2, the density for $Y_1 = A_1$ is retrieved. The following theorem has just been proven.

Theorem 3.2: Suppose v contains a normal background given by Eq. (3.2). Then the density of the signal coefficient A_1 is normal, and is given by $n(Y_1|\nu_1, \Psi_{11})$, where $\nu_1 = w^* \mu$, and $\Psi_{11} = w^* \Sigma^* w$.

Theorem 3.2 may now be used to formulate of the probability of detection. In section 2, Proposition 2.2 showed that if the background was smooth in space and time and no signal was present, then the signal coefficient, A_1, is equal to zero. It is easy to see by using a similar computation that if the signal is present in the absence of any background, $A_1 = 1$. For a signal in a target that is random, $Y_1 \equiv A_1$ is a RV, and in general, will be somewhere between 0 and 1. Detecting whether a signal is present, therefore, requires a thresholding operation on the RV Y_1. That is, after the vector v is convolved with w, the thresholding hypothesis is:

If $Y > t$, then a signal is present

If $Y < t$, then a signal is absent.

An optimal threshold τ is determined by comparing the PFA (the probability of detecting a target when none is present) with the probability of misdetection (the probability that a target is not detected when one is present). Here we are only interested in PFA in terms of the filter coefficients.

Since the threshold density corresponding to the RV Y_1 is given in terms of the weight vector a and correlation matrix, the probability of exceeding a given threshold may be computed. Let $n(Y_1|\nu_1, \Psi_{11})$ denote the density of the RV Y_1 having mean ν_1 and variance Ψ_{11}. The expressions for ν_1 and Ψ_{11} are given in Theorem 3.2. The probability that Y_1 is greater than a given threshold τ is:

$$\begin{aligned} Pr[Y > \tau] &= 1 - Pr[Y < \tau] \\ &= 1 - \int_{-\infty}^{\tau} n(Y|\nu_1, \Psi_{11})\, dY \end{aligned} \tag{3.18}$$

We may assume that ν_1 is zero, and let $\sigma^2 = \Psi_{11}$. Then

$$Pr[Y>\tau] = 1 - \frac{1}{\sqrt{2\pi}\sigma}\int_{-\infty}^{\tau} e^{\frac{-y^2}{2\sigma^2}} dy$$
$$= \frac{1}{2}\left[1 - Erf\left(\frac{\tau}{\sqrt{2}\sigma}\right)\right] \tag{3.19}$$

where Erf(x) denotes the error function at x. Using Theorem 3.2, Ψ_{11} can be written in terms of the weights and the FAR may be written as

$$Pr[Y>\tau] = \frac{1}{2}\left[1 - Erf\left(\frac{\tau}{\sqrt{2\,(w^* \Sigma^* w)}}\right)\right] \tag{3.20}$$

Equation (3.20) gives the PFA in terms of the weights and background statistics. Notice that if a filter is designed which does not match the target exactly, then a perturbation analysis may be done to determine how the PFA changes. (See Schwartz, 1990.)

4.0 Iterated Function Systems - An Introduction:

In the next section, we consider modeling backgrounds which fail to be smooth in one- dimension. By nonsmooth, we will mean any curve that is continuous, but which may be non-differentiable. The curve may also be scale invariant, such as a fractal curve. Iterated function systems (IFS) will be used throughout this section and the next, so we discuss the basic theory of IFS first. (The reader should consult Barnsley (1988) for a more detailed description.)

Let K be a compact set in R^2 supplied with a metric $d(\circ, \circ)$. Let w_i: $(K \rightarrow K)$ for i=1,...,N be strict contractions; i.e. there exists a positive constant s<1 such that

$$d(w_i(x), w_i(y)) \leq s\,d(x, y) \tag{4.1}$$

for all x,y ϵ K and i = 1,...,N. We define {K,w_i:i=1,...,N} to be an IFS [Barnsley, 1986]. The basic result states that there is a unique compact attractor $A \subset K$ such that

$$A = \cup w_i(A) \tag{4.2}$$

To see that A is an attractor, assume we are given an arbitrary point x_0 in K. Generate x_1 by the rule

$$x_1 = w_i(x_0) \text{ with probability } p_i \tag{4.3}$$

That is, associated with every map w_i, there is a number (namely a probability) p_i such that $0 < p_i < 1$, and $\sum_{i=1}^{N} p_i = 1$. Attractor A may be computed by using Eq. 4.3 and a random number generator. If there were only two maps (N=2), then each iteration could be determined by the flip of a coin, where $p_1 = p_2 = 1/2$.

The above technique generates an attractor with a certain distribution which depends on the probabilities chosen for each map. In applying the techniques of IFS, we require the location of the attractor at a set of pre-determined points. Therefore, we consider a deterministic generation of the attractor to an IFS. Since A is an attractor of a dynamical system, it must be a fixed point of the IFS. To see that this is so, define H to be set of nonempty compact subsets of K supplied with the Hausdorff metric

$$h(B,C) = max\left\{ \begin{pmatrix} max \\ x\epsilon B \end{pmatrix} \begin{pmatrix} min \\ y\epsilon C \end{pmatrix} d(x,y), \begin{pmatrix} max \\ y\epsilon C \end{pmatrix} \begin{pmatrix} min \\ x\epsilon B \end{pmatrix} d(x,y) \right\} \tag{4.4}$$

for all B,C ε H. Define $W: (H \rightarrow H)$ by

$$W(B) = \cup w_i(B) \tag{4.5}$$

Then W is a strict contraction with

h(W(B),W(C)) < s h(B,C) for all B,C ε H.

By the contraction mapping theorem [Barnsley,1988], it can be shown that A is the unique fixed point of W; i.e., A = W(A).

In contrast to the probabilistic iterative scheme given above, the set A may be computed deterministically as follows:

Choose A_0 ε H arbitrarily.

Let $A_{n+1} = W(A_n)$, n = 1,2,3,...

Then

$$A = \lim_{n \rightarrow \infty} A_n \tag{4.6}$$

Now we apply the IFS theory to a scalar function of a single variable.

5.0 Modeling and filtering unknown backgrounds in terms of IFS.

As mentioned in the previous sections, the matched signal detection problem deals with a signal in an unknown background. As such, a background model must be assumed in order to derive a filter. (In this case, the filter is assumed to be linear.) When the background model is assumed to be expandable in a Taylor series about some neighborhood, it is implicitly assumed that the background is highly correlated. Furthermore, the neighborhood considered is the defined length scale of the background. That is, the background cannot be modelled any more accurately using a larger number of samples. However, if the background has no real length scale, as is the case in many physical instances (see for example, Pentland, 1984), then a finite Taylor series expansion just averages over the samples without taking into account any of the scale invariant features. An explicit example of such a scale invariant background is the well-known Weierstrass function, defined by

$$B(x) = -\sum_{j=1}^{\infty} \lambda_y^{-1} \cos(2\pi\lambda_x^{j-1} x), \; x \in [-1,1], \tag{5.1}$$

where $\lambda_x > \lambda_y > 1$. Notice, if the derivative of the function B(x) is computed formally, it diverges, so that it is differentiable nowhere. Also, it can be shown that the capacity, or fractal, dimension of B(x) is given by $d_c = 2 - \frac{Ln(\lambda_y)}{Ln(\lambda_x)}$ (McDonald,1985). Natural backgrounds themselves may exhibit such behavior, as found in the work of Elgar (1989) and Lovejoy [1982], where oceans, clouds and rainfall have fractal dimensions. Therefore, one would like a more general model of the background in order to handle many different kinds of natural phenomena.

To this end, extensive use will be made of IFS-based models of the background. The model will be restricted to scalar valued functions of one variable. Let $I \equiv [x_0, x_N]$, and $I_n = [x_{n-1}, x_n]$, n = 1,2,3,...,N. The background is assumed to be continuous, and assumes the values y_i at the points x_i. For the present, assume the background is known. We follow Barnsley[1986] in designing an interpolation function based on IFS theory. Let $L_n: (I \rightarrow I_n)$ be defined by

$$L_n(x) = x_{n-1} + \frac{(x - x_0)(x_n - x_{n-1})}{x_N - x_0} \tag{5.2}$$

Clearly, the endpoints satisfy the conditions

$$\begin{aligned} L_n(x_0) &= x_{n-1} \\ L_n(x_N) &= x_n \end{aligned} \tag{5.3}$$

The explicit model of the background is now given. Let $-\infty < a < b < \infty$, and define the compact set $K \equiv Ix\,[a, b]$. Let $F_n\,(:K \rightarrow [a, b])$ be given by

$$F_n(x, y) = \alpha_n y + \beta_n x + \gamma_n \tag{5.4}$$

where $|\alpha_n| < 1$, β_n and γ_n are to be determined. We remark that although F_n is linear in both x and y, it need not be. The function F_n is defined such that

$$\begin{aligned} F_n(x_0, y_0) &= y_{n-1} \\ F_n(x_N, y_N) &= y_n \end{aligned} \tag{5.5}$$

For each n =1,2,3,...,N, Eq. (5-5) defines β_n and γ_n in terms of α_n.

The IFS for the background is defined by $\{K, W_n: n=1,2,3,...,N\}$, where W_n is given by

$$W_n\begin{bmatrix} x \\ y \end{bmatrix} = \begin{bmatrix} L_n(x) \\ F_n(x, y) \end{bmatrix}. \tag{5.6}$$

It can be shown that iterations of the above IFS converge to the graph of a continuous function, namely, (x,f(x)) such that $f(x_i) = y_i$ (Barnsley,1986). One can generalize the above results to more general functions than those used in Eq. (5.4), but the piecewise linear formulation is sufficient for our purposes here. The IFS as defined is an alternative method for interpolating data. The attractor of the IFS is the graph of a continuous function that interpolates the data, and depends on a set of N parameters, namely, $\alpha_1, \alpha_2, \ldots, \alpha_N$. By assigning a probability to each map of the IFS, one can generate the graph by iterating the IFS using a random number generator.

The free parameters $\alpha_1, \alpha_2, \ldots, \alpha_N$ determine the dimension of the graph of the interpolating function. Notice that by setting $\alpha_n = 0, n = 1, 2, 3, \ldots, N$, the attractor of the IFS asymptotes to well known linear interpolation formula, given by

$$f(x) = y_{n-1} + \frac{x - x_{n-1}}{x_n - x_{n-1}} \cdot (y_n - y_{n-1}), \tag{5.7}$$

n = 1,2,3,..., N. For the graph (x, f(x)) to be a fixed point of the IFS, it is a simple exercise to show that $F_n(x, f(x)) = f(L_n(x))$, where f(x) is defined by Eq. 5-7. Therefore, the dimension of the graph is 1.

When the α_n's are different from zero, the graph of f(x) will still interpolate the data points, but may not have an integer dimension. By noninteger dimension, we mean the ca-

pacity, or fractal dimension, which is defined as follows. Let ε be the length of a side of a box in R^2, and let G denote a set in R^2 that is bounded. Let $N(\varepsilon)$ be the number of boxes having side ε needed to cover set G, and define

$$d_c(\varepsilon) = \frac{\log(N(\varepsilon))}{\log\left(\frac{1}{\varepsilon}\right)}. \tag{5.8}$$

Then the capacity is defined as

$$d_c = \lim_{\varepsilon \to 0} d_c(\varepsilon). \tag{5.9}$$

To see what effect the parameters α_n have on the attractor of the IFS, consider the following interpolation problem. Let the unit box be denoted by $R_0 = [0,1]x[0,1]$, and let the interpolation points be (0,0), (1/2,1), (1,0). Let $w_i(x,y)$, i = 1,2 denote two of the maps defined by Eqs. 5.3-6. The area of R_0 is 1. To compute the number of boxes needed to cover the attracting set, we need to compute the areas of the successive iterates of the IFS on R_0. Since L_1 and L_2 map [0,1] to [0,1/2] and [1/2,1] respectively, each image has width equal to 1/2. However, since $|\alpha_1|, |\alpha_2| < 1$, the functions F_i, i=1,2 are both contracting in the y direction. (See Fig. 1 for an example of the image of R_0 where $\alpha_1 = 0.2$ and $\alpha_2 = 0.5$.) Therefore, after iterating once, the area of R_0 is reduced by each map by $\frac{1}{2}|\alpha_i|$, i=1,2, and the total area of the first iterate is

$$\frac{1}{2} \cdot [|\alpha_1| + |\alpha_2|] \tag{5.10}$$

After a second iterate (See Fig. 2.), applying each map to each sub-interval [0,1/2],[1/2,1] results in four new intervals each of length $\frac{1}{2^2}$, and the total area is now given by

$$\frac{1}{2^2} \cdot [|\alpha_1| + |\alpha_2|]^2. \tag{5.11}$$

Repeating the process n times results in an area equal to

$$\frac{1}{2^n} \cdot [|\alpha_1| + |\alpha_2|]^n \tag{5.12}$$

Assuming $|\alpha_1| + |\alpha_2| > 1$, and letting $\varepsilon = \frac{1}{2^n}$, then the total number of boxes needed to cover the n^{th} iterate of R_0 is

$$\frac{[|\alpha_1| + |\alpha_2|]^n}{2^n} \cdot 2^{n+1} = [|\alpha_1| + |\alpha_2|]^n \cdot 2. \tag{5.13}$$

It follows that

$$d_c(\varepsilon) = \frac{n\log\{2[|\alpha_1| + |\alpha_2|]\}}{(n+1)\log 2} \tag{5.14}$$

and

$$d_c = 1 + \frac{\log[|\alpha_1| + |\alpha_2|]}{\log 2} \tag{5.15}$$

By applying a similar analysis for p maps, it can be shown that after n iterates on R_0, we have

$$d_c(\varepsilon) = \frac{n\log\{p[|\alpha_1| + \ldots + |\alpha_p|]\}}{(n+1)\log p}, \tag{5.16}$$

and,

$$d_c = 1 + \frac{\log[|\alpha_1| + \ldots + |\alpha_p|]}{\log p}. \tag{5.17}$$

In Eqs. (5.16 and 5.17)), it is assumed that $|\alpha_1| + \ldots + |\alpha_p| > 1$. The above analysis may be summarized by the following theorem. Sketches of the proofs may be found in (Barnsley,1986,1988).

Theorem 5.1 Let $\{R_2; W_n, n = 1,2,3,\ldots,N\}$ denote the IFS described above by Eqs. (5-2) to (5-6) and defined with respect to the data set $\{(x_n,y_n), n = 0,1,2,\ldots,N\}$. Assume that α_n, $n = 1,2,3,\ldots,N$ satisfies $0 \le |\alpha_n| < 1$. Then:

1. There exists a unique nonempty compact set $G \subset R^2$ such that

$$G = \bigcup_{n=1}^{N} W_n. \tag{5.18}$$

2. The set G is the graph of a continuous function $f: \left([x_0, x_N] \rightarrow R \right)$; i.e., $G = \{(x f(x)): x \in [x_0,x_N]$.

3. The function f(x) interpolates the data; i.e., $f(x_i) = y_i$, $i = 0,1,2,\ldots,N$.

4. If

$$\sum_{n=1}^{N} |\alpha_n| > 1 \tag{5.19}$$

then the capacity, d_c, of the set G satisfies

$$\sum_{n=1}^{N} |\alpha_n| \cdot a_n^{d_c - 1} = 1 \tag{5.20}$$

where $a_n = \dfrac{(x_n - x_{n-1})}{(x_N - x_0)}$. *Otherwise,* $d_c = 1$.

Notice that if the distance between any two adjacent points is equal, and $[x_0,x_N] = [0,1]$, then $\alpha_n = 1/N$ for all n and Eq. (5.20) is equivalent to Eq. (5-17) if N=p.

Examples of attractors using the IFS with probabilities are shown in Figs. 3-7. In all cases, two maps were used with equal probabilities of 1/2, and the functions generated by the maps interpolate the points (0,0), (1/2,1), and (1,0). Notice that in Fig. 4 where $\alpha_1=\alpha_2=0.25$, the attractor is the graph of the parabola given by $f(x) = 4(x-x^2)$. Indeed, it can be shown using the definitions of the maps W_1 and W_2 defined by Eq. (5-6) that

$$W_1\begin{bmatrix} x \\ f(x) \end{bmatrix} = \begin{bmatrix} \frac{x}{2} \\ f\left(\frac{x}{2}\right) \end{bmatrix}$$

$$W_2\begin{bmatrix} x \\ f(x) \end{bmatrix} = \begin{bmatrix} \frac{(x+1)}{2} \\ f\left(\frac{(x+1)}{2}\right) \end{bmatrix} \tag{5.21}$$

In Figs. 5-7, as α increases, the dimension increases and the graph takes on a rougher appearance. It is clear from this example that by varying α_1 and α_2, both smooth and fractal approximations of a given background can be made.

Now we make the more realistic assumption that the background is unknown. Specifically, our assumptions are:

A1) There is a signal s(x) known apriori that is to be detected.

A2) There is an observed signal, v(x).

A3) The background or noise source y(x) is unknown, and continuous.

A4) The observed signal is composed of the sum of a scaled signal s and the background y;i.e.,

$$v(x) = A \cdot s(x) + y(x) \tag{5.22}$$

A5) The functions s,v,y are all defined on $I = [x_0, x_N]$. Let s_i, v_i, and y_i denote the values $s(x_i), v(x_i)$, and $y(x_i)$. Since the constants β_n and γ_n in Eq. (5-4) need to be determined, by assumption A3 and Eq. (5-5) we need to solve the system of equations

$$\left.\begin{aligned} \alpha_n y_0 + \beta_n x_0 + \gamma_n &= y_{n-1} \\ \alpha_n y_N + \beta_n x_N + \gamma_n &= y_n \end{aligned}\right\}, n = 1, 2, 3, \ldots, N \tag{5.23}$$

Since the y_n's are unknown, assumption A4 implies that the system given by Eq. (5-23) has the 2N+1 unknowns A, (β_n, γ_n), $n = 1, 2, 3, \ldots, N$. The system to solve is introduced by the following notation. Let $p \in R^{2N+1}$ be defined by

$$p^t = (A, \beta_1, \gamma_1, \beta_2, \gamma_2, \ldots, \beta_N, \gamma_N) \tag{5.24}$$

and let $F: R^{N+1} x R^N \rightarrow R^{2N}$ be defined by

$$(F(s, \alpha))^t = (s_0 - \alpha_1 s_0, s_1 - \alpha_1 s_N, s_1 - \alpha_2 s_0, s_2 - \alpha_2 s_N, \ldots, s_N - \alpha_N s_0, s_N - \alpha_N s_N) \tag{5.25}$$

Let the 2x2 matrix X be given by

$$X = \begin{bmatrix} x_0 & 1 \\ x_N & 1 \end{bmatrix}. \tag{5.26}$$

Then Eq. (5-23) becomes

$$\begin{bmatrix} & X & & & \\ & & X & & \\ & & & X & \\ F(s, \alpha) & & & \circ & \\ & & & & \circ \\ & & & & & \circ \\ & & & & & & X \end{bmatrix} p = F(v, \alpha). \tag{5.27}$$

In Eq. (5-27), $s^t = (s_0, \ldots, s_N)$, $\alpha^t = (\alpha_1, \ldots, \alpha_N)$, and $v^t = (v_0, \ldots, v_N)$. Since s is a known vector by hypothesis A1, the coefficient matrix on the left-hand-side of Eq. (5-27) is a function of α only, and we may rewrite this system as

$$Z(\alpha) \cdot p = F(v, \alpha), \tag{5.28}$$

where Z is a 2N x 2N+1 matrix.

Since there are fewer equations than unknowns in Eq. (5-28), the system is underdetermined of rank 2N, which implies the existence of infinitely many solutions. A particular solution may be computed by minimizing the residual in the Euclidean norm;i.e., find **p** such that

$$\left(\begin{matrix} (min) \\ p \epsilon R^{2N+1} \end{matrix} \right) \| Z(\alpha) \cdot p - F(v, \alpha) \|_2 \tag{5.29}$$

The solution to Eq. (5-29) is found by solving the normal equation

$$Z^t(\alpha) \cdot [F(v, \alpha) - Z(\alpha) p] = 0. \tag{5.30}$$

Assuming the rank of Z(α) to be 2N, a unique solution p* may be found by constructing the singular value decomposition of Z(α) (Rao and Mitra [1971]); i.e., there exist unitary matrices, U and V, and a diagonal matrix D such that

$$Z(\alpha) = U[D\ 0]V^H \tag{5.31}$$

Indeed,

$$p^* = Z^{\perp}(\alpha) \cdot F(v, \alpha) \tag{5.32}$$

where $Z^{\perp}(\alpha)$ is the generalized Moore-Penrose inverse of Z.

The next proposition characterizes the basic properties of **p***. Its statement and proof are similar to those given in Section 2.

Proposition 5.2 Suppose Z(α) has full rank.

1. If v = s (Signal in the absence of noise), then $p^{*t} = (1, 0, 0, 0, \ldots, 0)$ *). The IFS model generates f(x)=0 for all* $x \in [x_0, x_N]$.

2. If v = y (no signal present, just noise), then $p^{*t} = (0, \beta_1, \gamma_1, \beta_2, \gamma_2, \ldots, \beta_N, \gamma_N)$ *, where the* β_n *and* γ_n *are those parameters for the IFS which interpolates the data set* $\{(x_n, y_n)$, $n=0,1,2,\ldots, N$.

Notice that since the scaling coefficient of the signal, A_1, is the first component of **p***, in the first part of the theorem there is a perfect match ($A_1=1$), while in the second part of the theorem, no detection of a signal is made ($A_1=0$). Design of a linear filter based upon the

IFS model of the unknown background is now given, the proof of which is straight forward.

Theorem 5.3 Let $z_{ij} = [Z^{\perp}]_{ij}$ *The signal amplitude A defined in hypothesis may be written as a discrete convolution:*

$$A = w^{*} v, \tag{5.33}$$

where the filter weights are given by an N+1 dimensional vector w:

$$\begin{aligned} w_0 &= z_{1,2N}(1-\alpha_N) - \sum_{j=1}^{N-1} z_{1,2j}\alpha_j \\ w_N &= z_{1,1}(1-\alpha_1) - \sum_{j=1}^{N-1} z_{1,2j+1}\alpha_{j+1} \\ w_j &= z_{1,2N-2j+1} + z_{1,2N-2j}, j = 1, 2, 3, \ldots, N-1 \end{aligned} \tag{5.34}$$

The above results dictate how to design a linear filter which detects a signal in a background that is continuous. If one solves the full system, thereby generating the parameters for the IFS, a model of the background can be generated as an attractor of the IFS. Furthermore, if there is no known length scale, Theorem 5.1 will yield the dimension of the background. In addition, the results of Theorem 5.3 when combined with Eq. (3.20) will yield the PFA for the weights based upon the IFS filter.

6.0 Numerical examples:

In this section, we give some simple examples of the IFS-based techniques. The technique of approximating backgrounds can be demonstrated by considering a sample signal array of 500 points, and the signal is assumed to contain a constant target. That is, the signal is background only with a constant offset. Figure 8a shows a sample background signal which was generated, having a maximum amplitude of 0.2. To this background, a constant background was added, having an amplitude of 1/2. (The offset is not shown.) Figure 8b shows the IFS prediction of the background only using only 10 maps at intervals of 0.1. The 10-dimensional parameter controlling the dimension, α, was chosen to minimize the residual error along the signal. The values of α used in predicting the background are (0.25, 0.8, 0.7, 0.5, 0.3, 0.2, 0.25, 0.8, 0.3, 0.4). The IFS predicted signal does well in approximating the actual signal except in the region between 0.4 and 0.7, where the characteristic shapes do not agree in shape. However, the amplitudes are in the same range. Improvements can be made by adding more maps, or, if information about the dimension

is known aprioi, a constraint can be added. From the figure, it is seen that only 10 parameters can be used to model 500 points.

When a signal is present, backgrounds may still be simulated by solving the relevant equations for β and γ in terms of the contraction constants α. In Figs. 9a and 9c, a ramp function is randomly embedded in a noisy signal which has a dimension approximately equal to 1.41. Figures 9b and 9d show the simulated signal generated by the IFS defined by the coefficients β and γ. Ten sub-intervals were used over each convolution length of 100 points, and α is chosen to take the same value for each subinterval. In Fig. 9b, the value of α was chosen to give the graph of the background a dimension of 1.41, while the dimension of the graph in Fig. 9d is equal to 1.95. Notice that by changing α so that the dimension increases, the simulated background in Fig. 9c becomes rougher and has more local wiggles. Extreme values of the simulated background having higher dimension are also larger.

To see the effect α has on the actual convolution of a filter designed using an IFS, we first examine a normal function having standard deviation of 1/2 as the signal to be detected. Signal plus noise is generated by adding the normal function to a noisy signal which has a bound of 25 percent noise and a dimension approximately equal to 1.4. Figure 10a shows such a signal. As before, only 10 sub-intervals were used for each convolution segment of 100 points, and α takes the same value on each subinterval. In Fig. 10b, α is chosen so the dimension of the background is 1.43. Notice that in addition to the signal being passed upon convolution, the noise is also passed. This is a result of the linearity of the filter, and the fact that the window is shifted point by point to the right along the signal. Because the known signal is smooth and the background is fractal, the noise might be considered almost orthogonal to the filter weight vector. This can be seen from Fig 10b since the noise is reduced in overall amplitude in intervals where the signal is absent. If α is increased so that the dimension of the simulated background is increased to 1.99, as is done in Figs. 10c and 10d, then negative trends in the convolution appear magnified. Overshoot in the convolved signal becomes dominant, and it is easy to see that many false signals might be passed through a threshold operation.

Returning to the ramp function, we now examine graphically how the convolution between the signal and filter behaves. Figures 11a and 11b depict the result of a convolution where α has been chosen to model a background with dimension of 1.41. Notice that because there is an increasing or decreasing trend in the background, the noise is amplified as well as the signal. That is, the filter tries to magnify the trends appearing as ramps in the noise. If the dimension of the modelled background is assumed to be higher, as is the case in Figs. 11c and d, convolution values of -1 may be achieved, along with noise amplification, implying the existence of a greater number of false alarms when a threshold is imposed. Given the appearance of the overshoot and noise amplification in the case of greatly differing dimension between the noise and modelled background observed in the

previous two examples, we conjecture this holds true in general for linear IFS-based filters. That is, if the signal is smooth, and the background fractal having a dimension d_b, there is a neighborhood about d_b in which the false alarm rate is relatively constant. Outside this interval, however, the false alarm rate increases. This idea will be pursued in detail elsewhere.

Finally, the results of applying a filter based upon a linear background model from Section 3 to a normal signal embedded in a large amplitude fractal background is presented in Fig. 12a and 12b. The background has dimension 1.4. The signal the filter is seeking is a normal curve with fixed standard deviation and random amplitude. Notice the overshoot of the filter to large negative values, which could lead to high PFA. In addition, there are many intervals in which the filter says the signal is there, but in reality it is not, leading to a very high false alarm rate. The fractal based filter for the same signal is shown in Figs. 12c and 12d, where the dimension of the background model is equal to the dimension of the imposed background. Not only does the filter detect the signal location correctly, it also gets the relative amplitudes correct. The overall noise is greatly reduced, yielding a filtered signal with a much improved signal to noise ratio. The original signal in the absence of any noise is depicted in Fig. 12e.

7.0 Summary:

We have given a derivation of an LMS filter using a least mean squares technique based upon *smooth and nonsmooth (fractal)* background noise sources. Backgrounds which are unknown may be modelled using smooth or fractal functions. The filter is designed as a linear convolution based upon a known signal, and may implemented in a detection mode by using a particular thresholding operation. It was shown that the convolution with a given background upon which the filter was designed results in a nulling operation, while convolving the filter with the known target in the absence of any noise results in the signal coefficient having a value of unity. This implies that the filter can be used in a threshold operation for the signal detection problem. The operation of the filter in a Gaussian background was considered, and a FA probability was derived.

Fractal backgrounds were considered, and a technique based upon IFS was used to model them. Currently, the dimension is set as a free parameter, determined by the choices of the contraction constants for the IFS. Simulation of unknown fractal backgrounds using the IFS as a model may be done using a small number of parameters. The advantage is that fewer points are needed to design a filter which operates on a signal in a structured background.

Since this paper only addresses how to design a matched filter using IFS-based models of the background, much work needs to be done in specifying performance issues using vari-

ous known metrics. Under the current assumptions, the signal is stationary, so one expects parameter dependent quantities like scale-invariance or dimension to remain constant. Therefore, LMS techniques can be used to find a vector contraction parameter, α, to minimize some least square error in the residual error. To perform such an operation requires the computation of changes in the attractors of the IFS to small changes in parameters. This may be done in parallel using the techniques of Withers [1987], and will be reported on elsewhere.

The techniques of filter design using smooth backgrounds may also be extended to fractal backgrounds. In sections 1,2, and 3, a linear superposition of smooth basis functions was used. However, one may also use the same superposition in modeling fractals using wavelets [Argoul et al, 1989; Holschneider, 1988; Morlet et al, 1982, I, II].

The problem of non-stationarity may be dealt with by using adaptive filtering, and by measuring the dimension and using it as a constraint in designing the filter. Of course, this is longer to compute in practice, but if many samples are taken over a particular ensemble, the dimension sought after may be found which optimizes performance. Other extensions are those to higher dimensions, and these will be reported elsewhere.

Finally, by applying fractal-block coding techniques such as those in [Jacquin,1990] to the unknown background, one can automate the design of the filter and the model of the unknown background entirely.

REFERENCES

F. Argoul, A. Arneodo, G. Grasseua, Y. Gagne, E. J. Hopfinger, and U. Frisch, "Wavelet analysis of turbulence reveals the multifractal nature of the Richardson cascade," Nature (London) 338, pp.51-53 (1989).

G. I. Barenblatt and I. A. Leykin, "On the self-similar spectra of wind-waves in the high frequency range," Izv. Acad. Sci. USSR Atmos. Oceanic Phys. **17**, pp.35-41 (1981).

Michael Barnsley, Fractals Everywhere, Academic Press, Inc., Boston, 1988.

Barnsley, Fractal functions and interpolation, Constr. Approx., 2 (1986), pp.303-329.

M. Ausloos and D. H. Berman, "A multivariate Weirstrass-Mandelbrot function," Proc. R. Soc. London Ser A. 400, p. 331-350 (1985).

David Shi Chen, A data-driven intermediate level feature extraction algorithm, IEEE Trans. Pattern Anal. and Machine Intell., 11(1989), pp. 749-758.

S. Elgar and G. Mayer-Kress, Observations of the fractal dimension of deep- and shallow-water ocean surface gravity waves, Physica D, 37(1989), pp.104-108.

K. J. Falconer, *The Geometry of Fractal Sets*, Cambridge University Press, Cambridge (1985)

W. A. Gardner, Introduction to Random Processes: with Applications to Signals and Systems,Macmillan Publishing Co., New York, 1986.

M. Holschneider, "On the wavelet transformation of fractal objects," J. Stat. Phys. **50,** pp. 963- (1988).

R. Hecht-Nielson, Nearest matched filter classification of spatiotemporal patterns, Applied Optics, 26(1987), pp.1892-1899.

B. D. Hughs, M. F. Shlesinger, and E. W. Montroll," Random walks with self-similar clusters," Proc. Nat. Acad. Sci., 78(1981).pp.3287-3291.

A. E. Jacquin, "Image coding based on a fractal theory of iterated contractive image transformations,", preprint (1990).

T. Kalaith, A view of three decades of linear filtering theory, IEEE Trans. Information Theory, IT-20 (1974), pp.148-181.

M.S. Longmire and E. H. Takken, LMS and matched digital filters for optical clutter suppression, Applied Optics, 27(1988),pp.1141-

S. Lovejoy, "The area-perimeter relationship for rain and cloud areas," Science, **216**(1982),pp.185-187.

S. Lovejoy and B. B. Mandelbrot, "Fractal properties of rain, and a fractal model," TELLUS, 37a(1985), pp.209-232.

S. Lovejoy and D. Schertzer, "Scale invariance, symmetries, fractal, and stochastic simulations of atmospheric phenomena," Bull. Am. Met. Soc., 67(1986), pp.21-32.

Stephane G. Mallat, A theory for multiresolution signal decomposition:The wavelet representation, IEEE Trans. on Pattern Analysis and Machine Intelligence, 11(1989), pp. 674-693.

S.W McDonald, C. Grebogi, E. Ott, and J.A. Yorke, Fractal Basin Boundaries, Physica 17D (1985), pp.125-153.

J. Morlet, G. Arens, E. Fourgeau, and D. Goird, "Wave propagation and sampling theory-Part I: Complex signal and scattering in multilayered media," Geophysica 47,pp. 203-221 (1982)

J. Morlet, G. Arens, E. Fourgeau, and D. Goird, "Wave propagation and sampling theory-Part II: Sampling theory and complex waves," Geophysica47,pp.222-236, (1982)

Thomas S. Parker and Leon O. Chua, Chaos: A tutorial for engineers, Proceedings of the IEEE, 75(1987), pp.982-1008.

Alex P Pentland, Fractal-based description of natural scenes, IEEE Trans.

on Pattern Analysis and Machine Intelligence, 6(1984), pp.661-674.

W. K. Pratt, Digital Image Processing, Wiley, New York (1978).

C. R. Rao and S. K. Mitra, Generalized Inverse of Matrices and its Applications, John Wiley and Sons, New York (1971).

I. Reed, R. Gagliardi, and L. Stotts, Optical moving target detection with 3-D matched filtering, IEEE Transactions on Aerospace and Electronic Systems, 24(1988), pp.327-336.

I. B. Schwartz, "Derivation and analysis of a least mean square filter," Math. Comp. Modelling, 13, pp.37-44 (1990).

I. B. Schwartz, The Least Means Square Filter: A probabilistic approach, (1990) to be published.

D. A. Scribner, I. B. Schwartz, D. Ilg, J. Havlicek, M. Pauli, G. Katz, and R. Priest, 3-D LMS filtering techniques for detection of moving targets against clutter backgrounds, IRIS proceedings on Target and Background Discrimination, in press.

M. C. Stein, Fractal image models and object detection, SPIE, 845(1987),

pp.293-300.

M. Stiassne, Dept. of Applied Mathematics, California Institute of Technology, Pasadena, CA 91125, "The fractal dimension of the ocean surface," preprint, (1986).

N. G. van Kampen, Stochastic Processes in Physics and Chemistry, North-

Holland, Amsterdam, 1981.

H.L. van Trees, Detection, Estimation, and Modulation Theory, John Wiley

and Sons, New York, 1968.

B. J. West and M. F. Shlesinger, "On the ubiquity of 1/f noise," Int. J. Mod. Phys. B. 3, pp. 795-820 (1989).

W. D. Withers, Calculating derivatives with respect to parameters in iterated function systems, Physica D 28,pp. 206-214.

E. Wong and B. Hajek, *Stochastic processes in Engineering Systems*, Springer-Verlag, New York, 1985.

G. M. Zaslavskii and E. A. Sharkov, "Fractal properties of breaking zones of sea surface waves," Sov. Phys. Dokl., 32 (1987), pp.499-501.

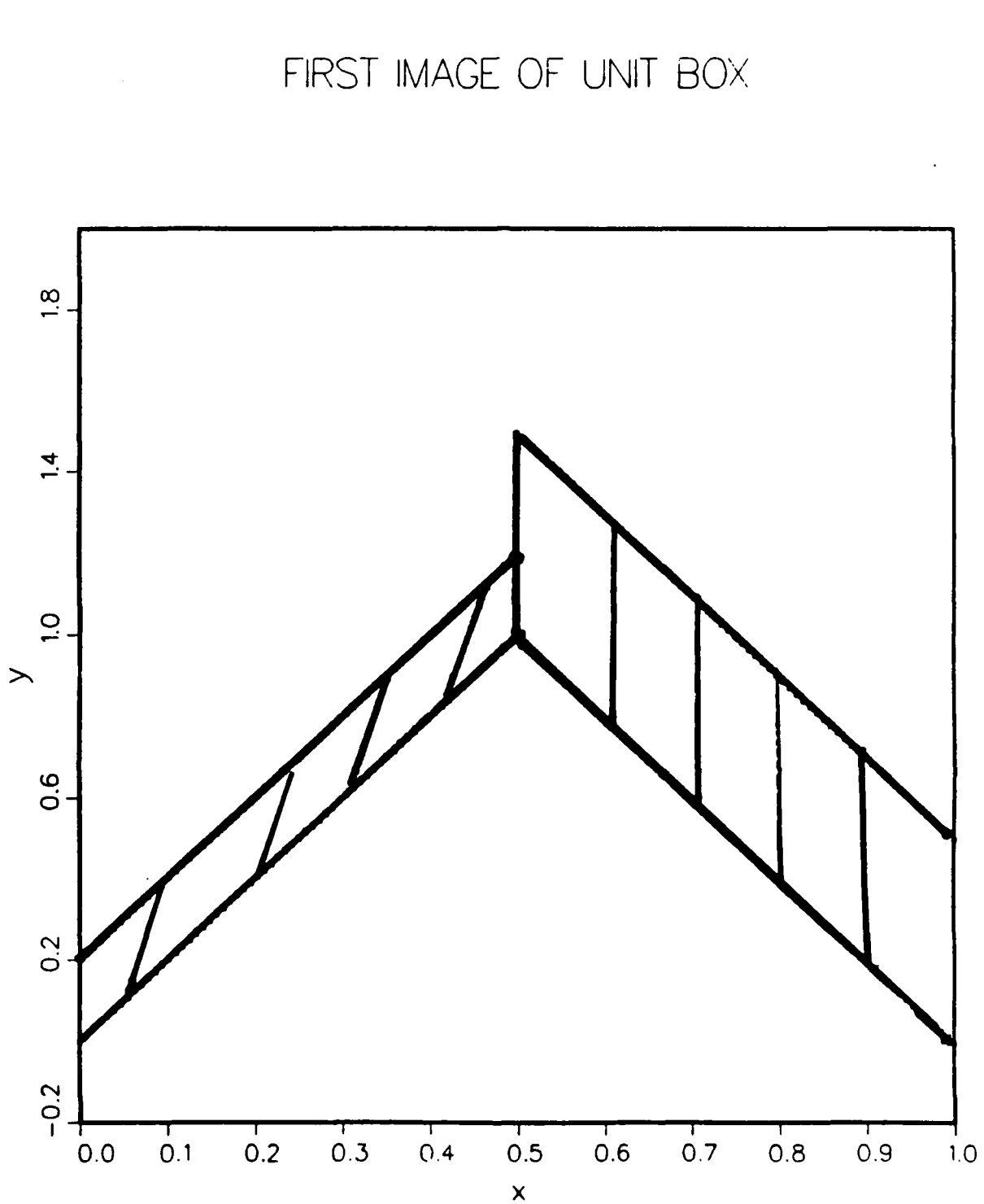

Fig. 1 — Shaded image is the first image of the unit box where $\alpha_1 = 0.2$ and $\alpha_2 = 0.5$.

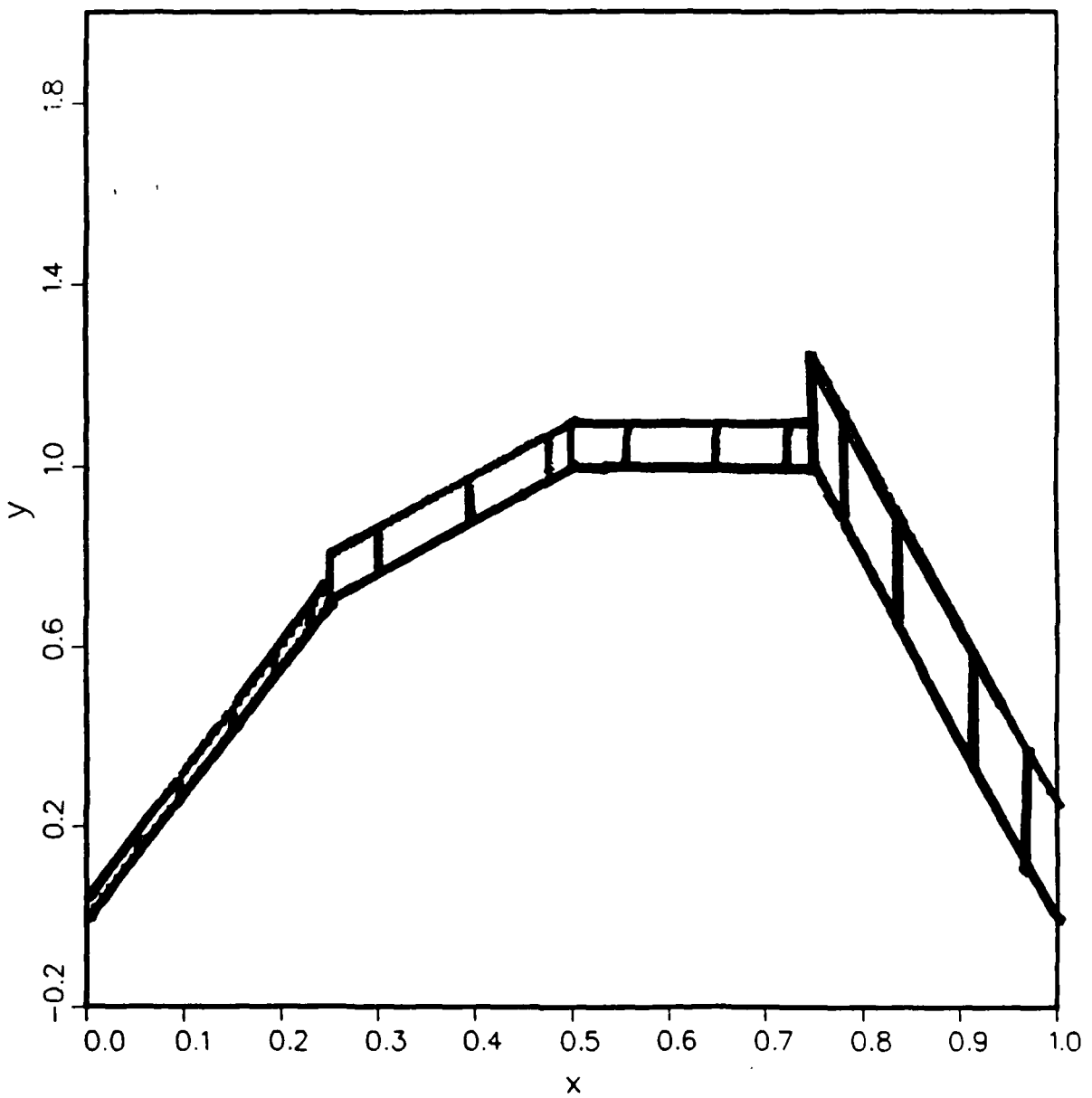

Fig. 2 — Same as Fig. 1, but the shaded region is the second image of the unit box

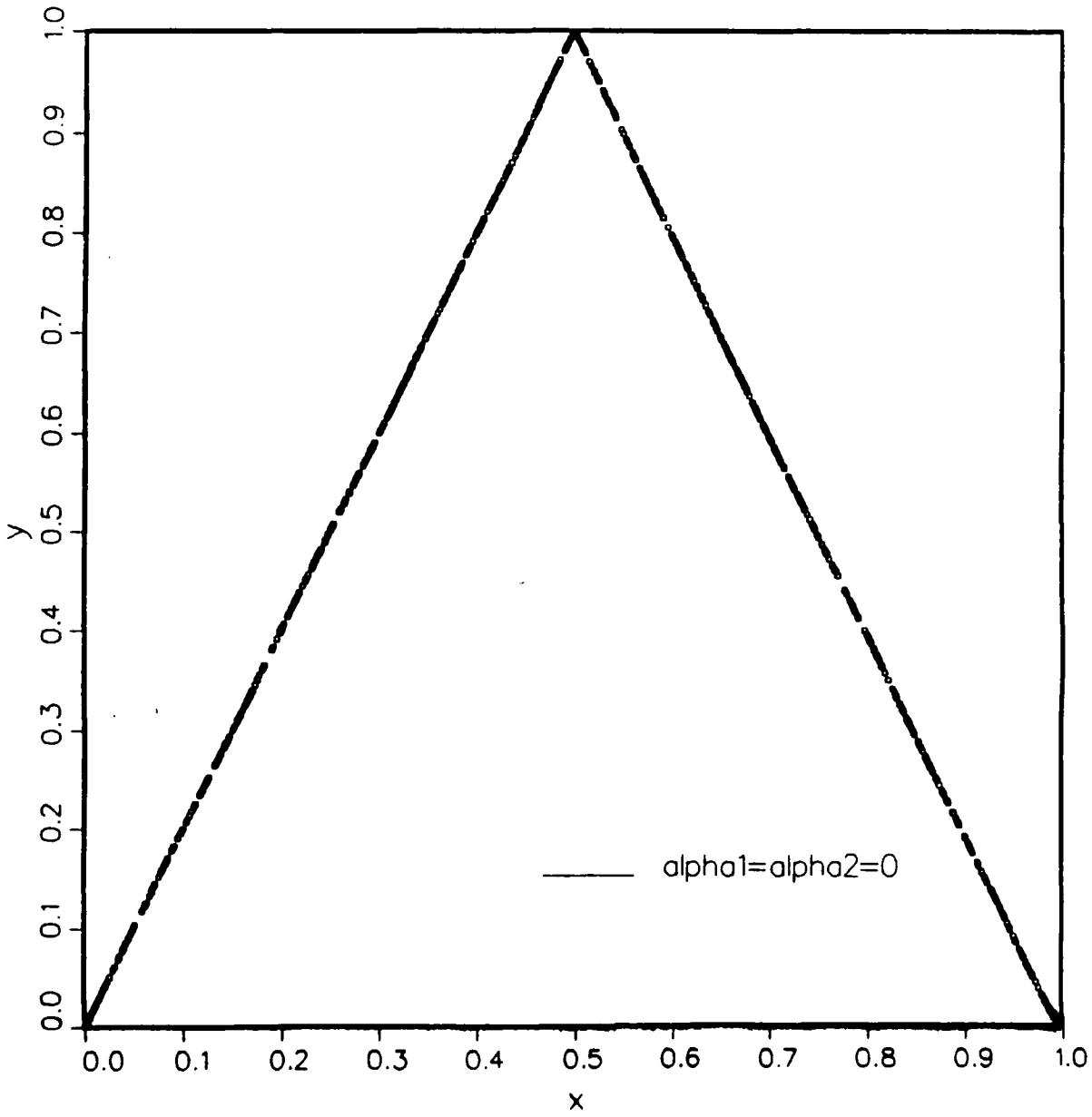

Fig. 3 — The attractor of the IFS which interpolates the points (0,0), (1/2, 1), and (1.0). $\alpha_1 = \alpha_2 = 0$.

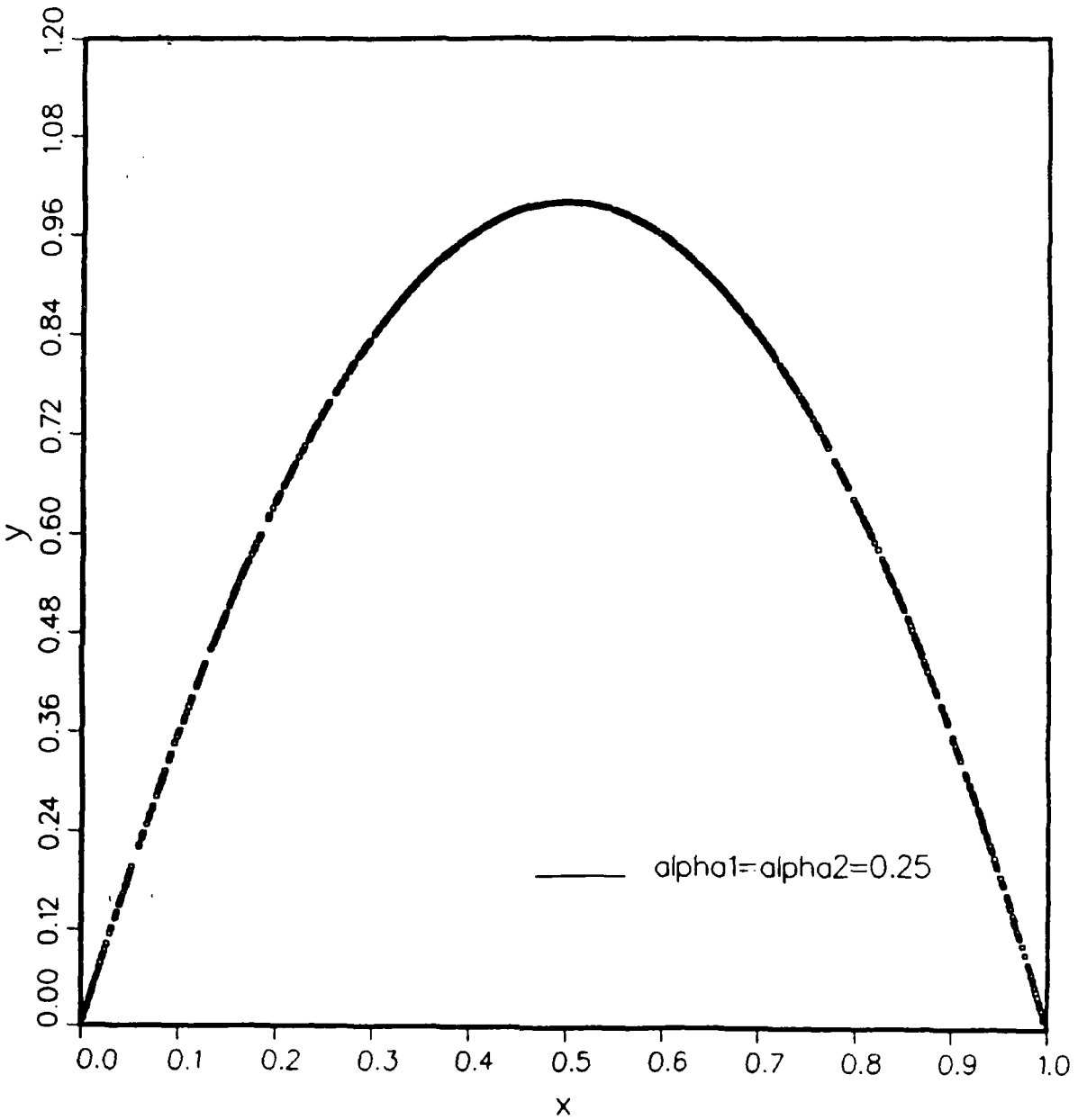

Fig. 4 — Same as Fig. 3, except $\alpha_1 = \alpha_2 = 0.25$

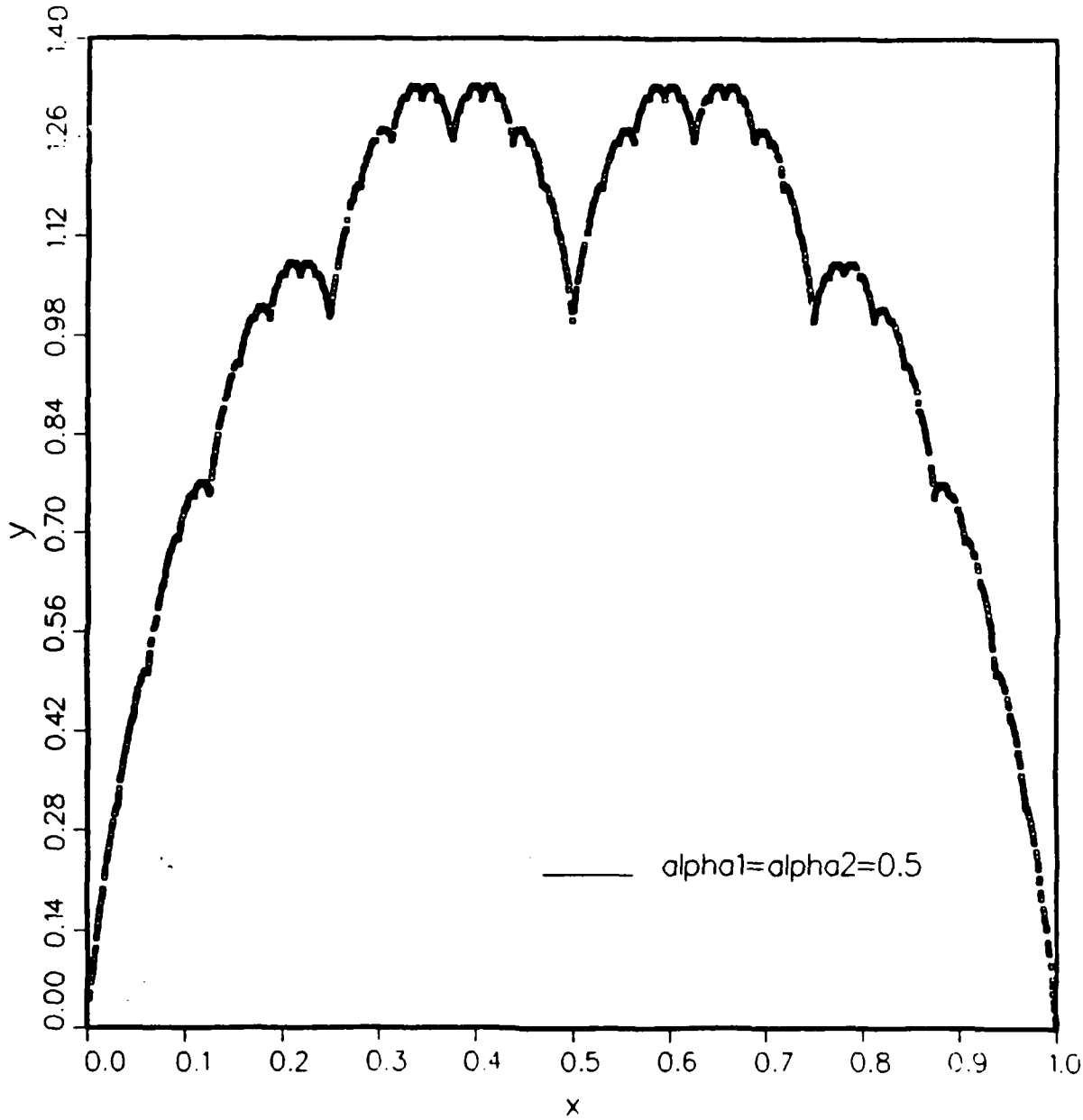

Fig. 5 — Same as Fig. 3, except $\alpha_1 = \alpha_2 = 0.5$

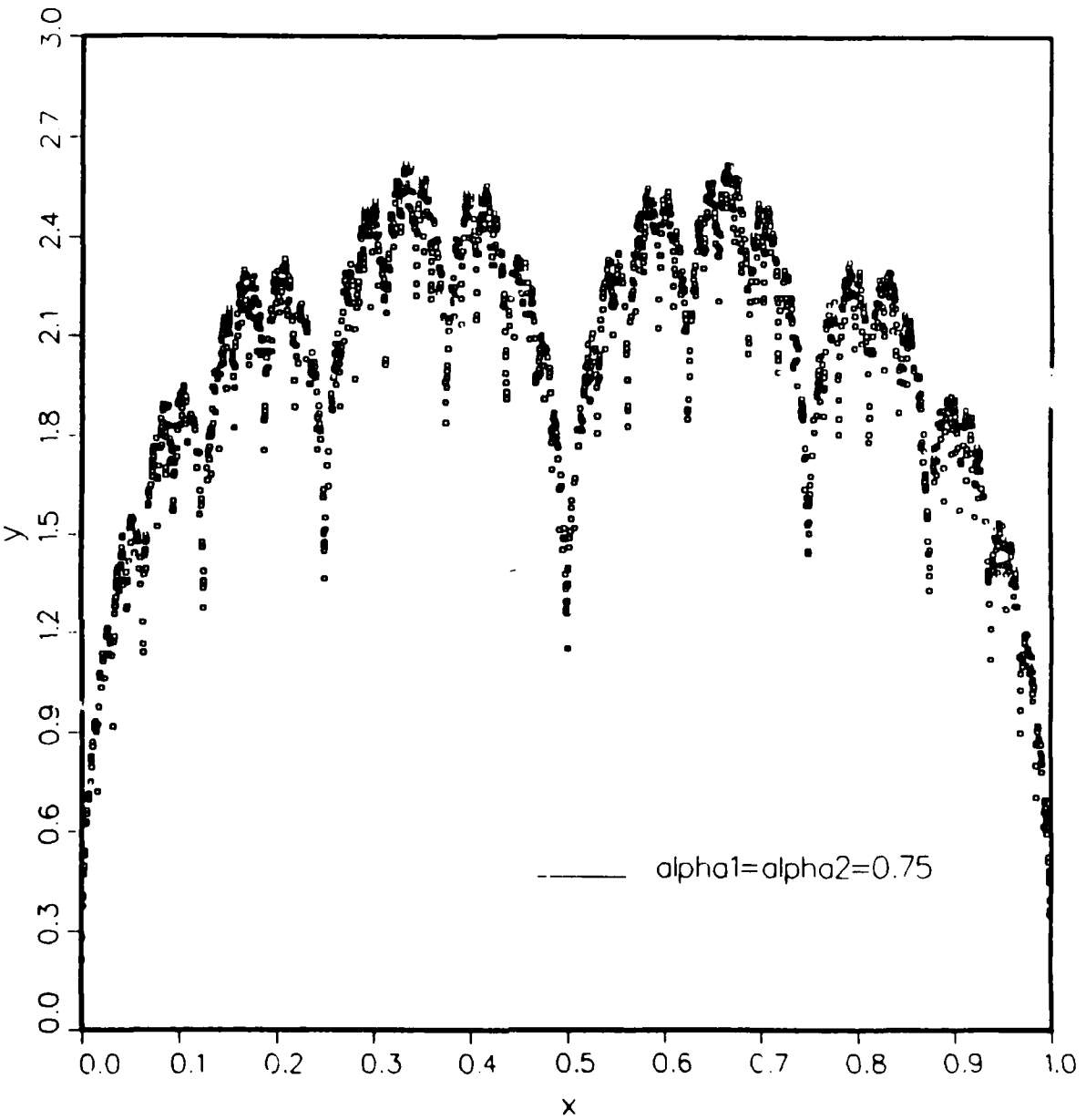

Fig. 6 — Same as Fig. 3, except $\alpha_1 = \alpha_2 = 0.75$

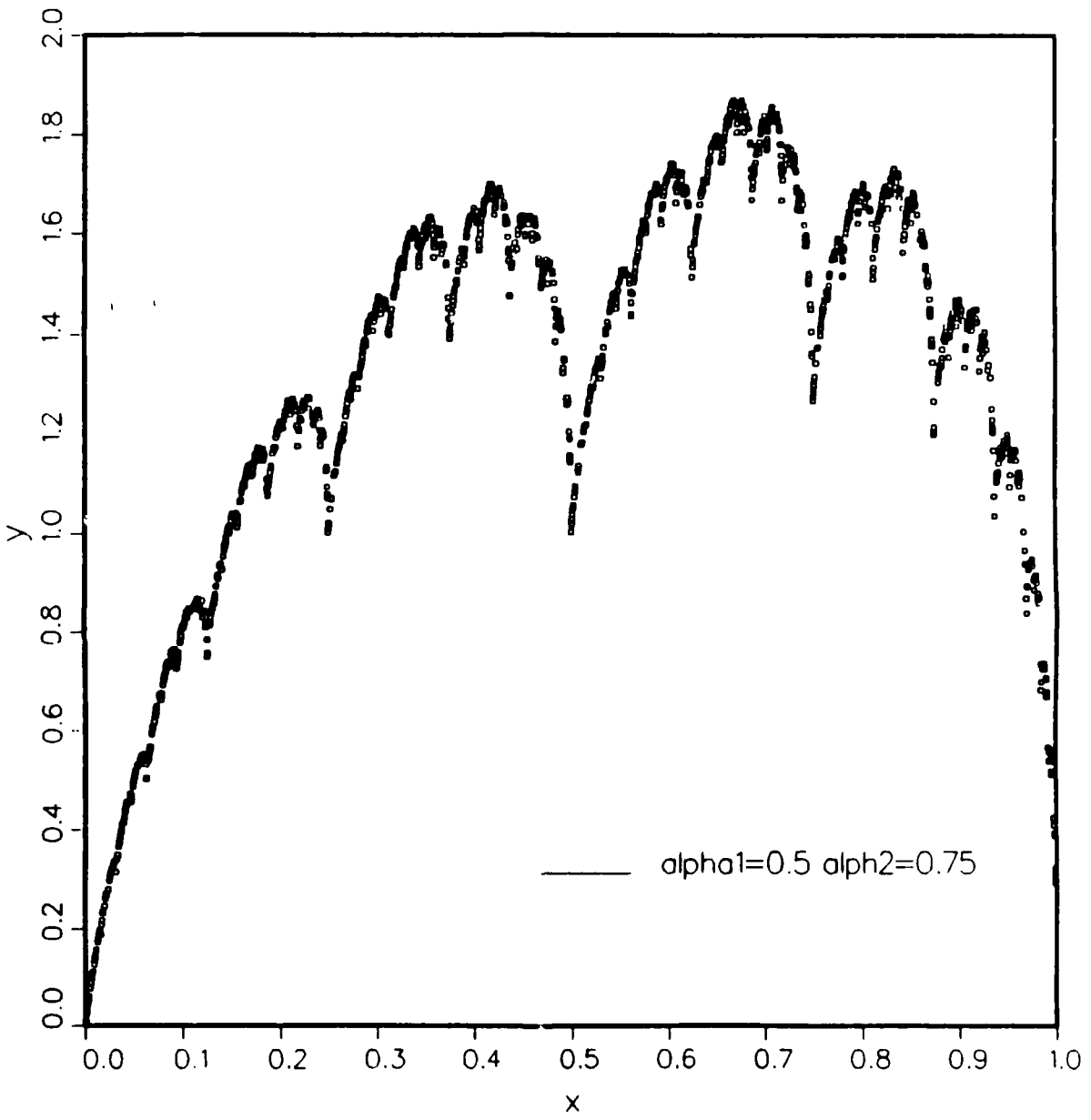

Fig. 7 — Same as Fig. 3, except $\alpha_1 = 0.5$, $\alpha_2 = 0.75$

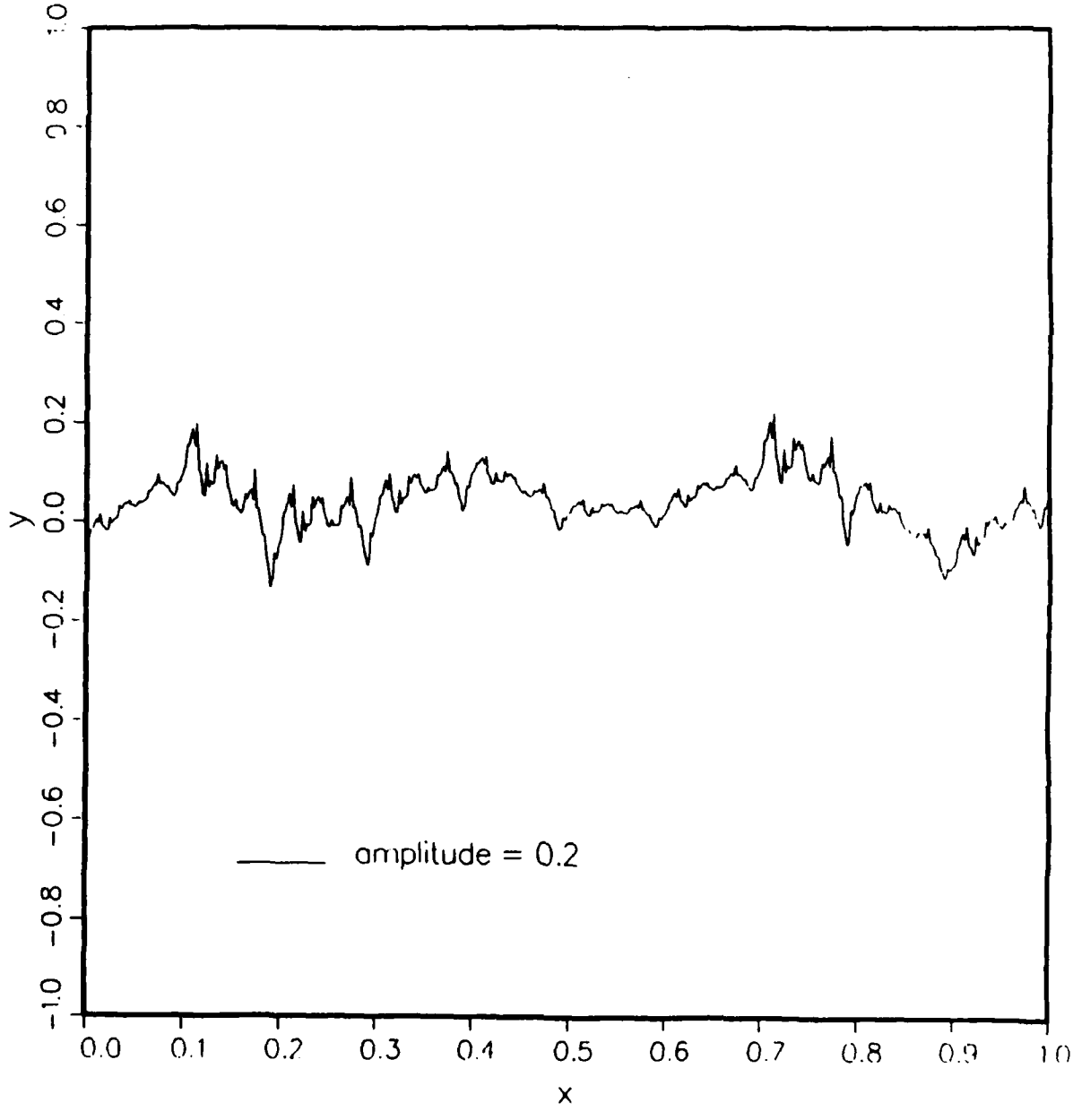

Fig. 8a — Sample noise having dimension $d = 1.65$

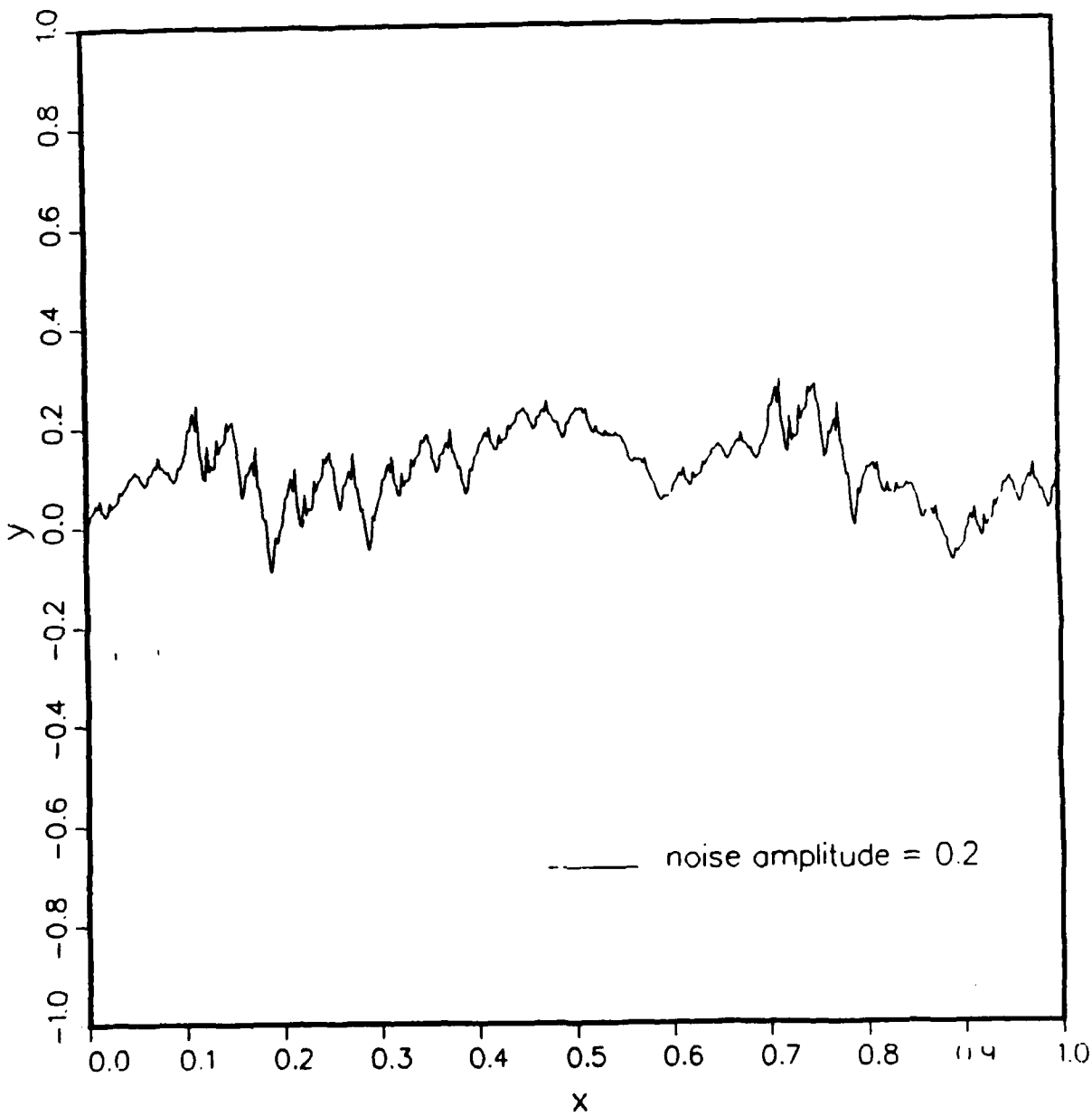

Fig. 8b — Predicted noise using 10 contraction parameters. The Sample noise in Fig. 8a was offset by a constant signal of 1/2.

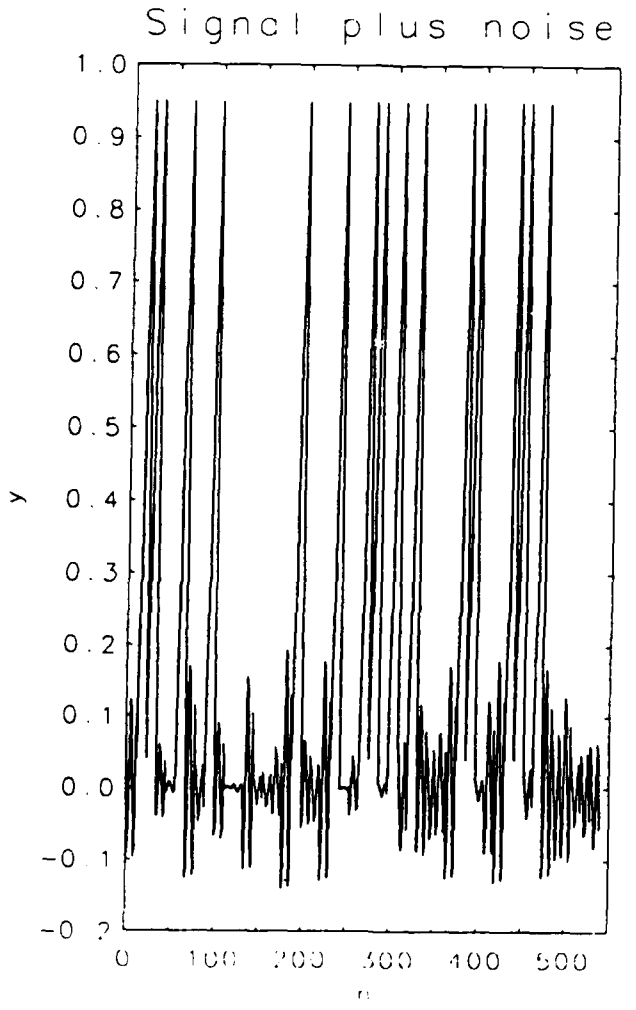

Fig. 9a — Signal plus noise, where the dimension of the noise is approximately 1.41. The signal used is a ramp function.

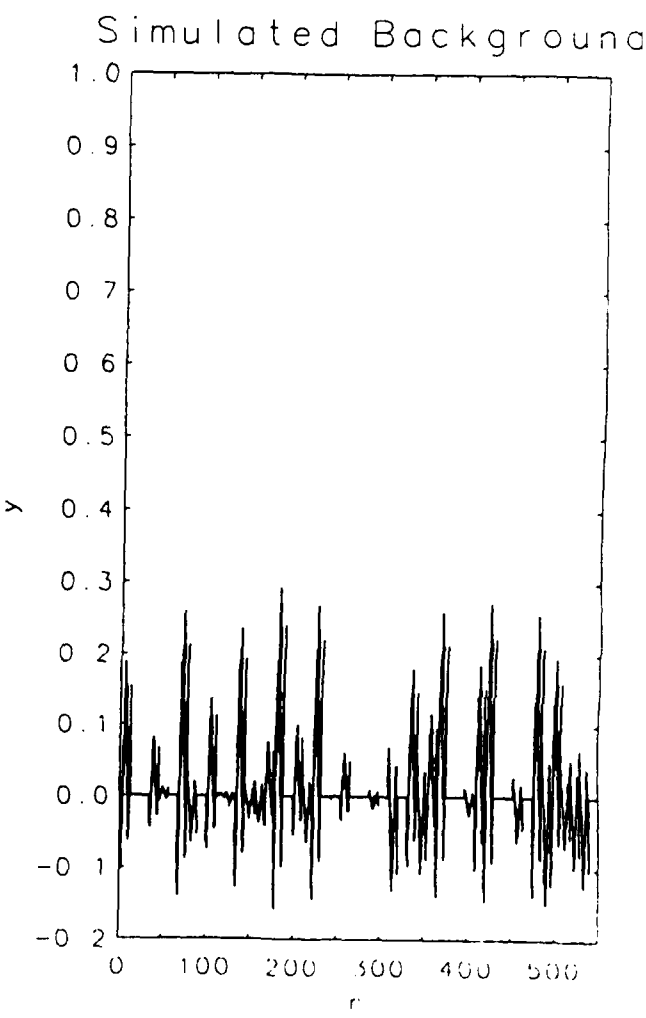

Fig. 9b — Modelled noise based on the IFS model using the LMS technique. Dimension of noise is 1.4

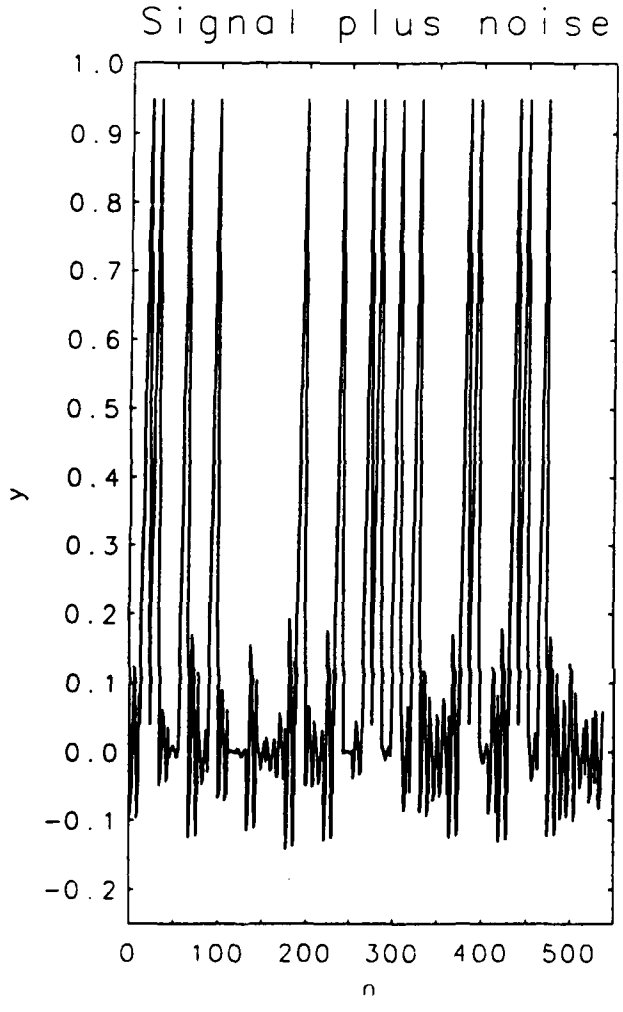

Fig. 9c — Same as Fig. 9a

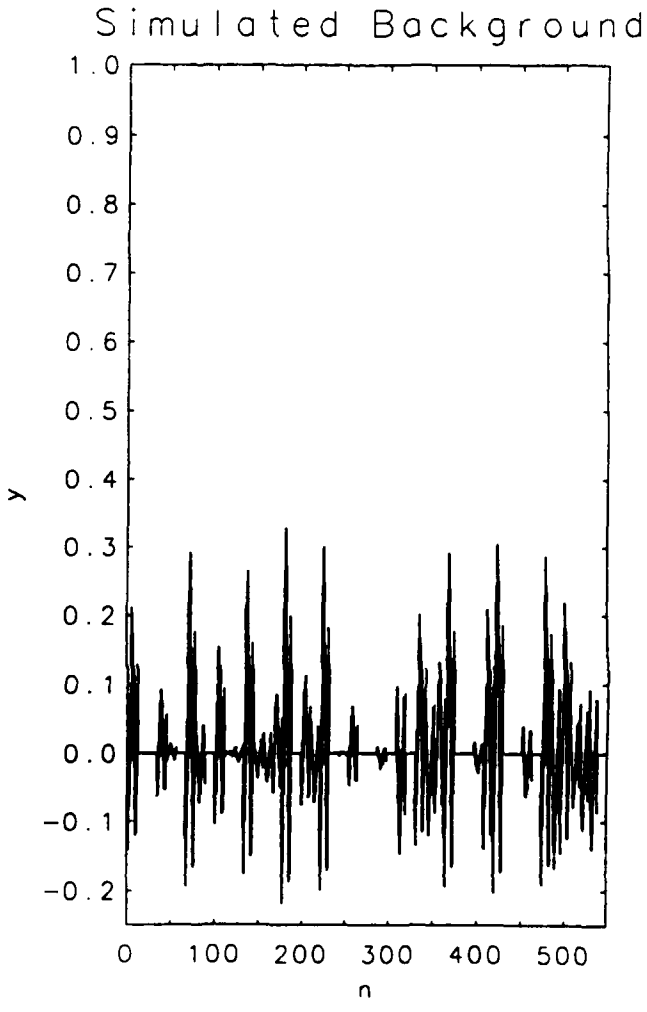

Fig. 9d — Same as Fig. 9b, except the parameter α is chosen so that the dimension is 1.95

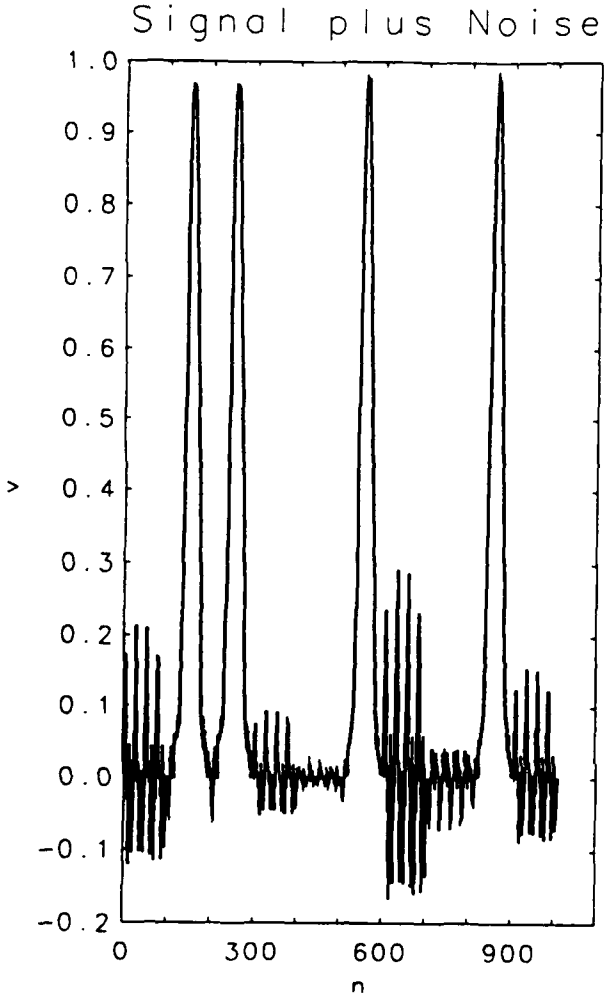

Fig. 10a — Same as Fig. 9a, except the known signal to be detected is a normal function having standard deviation of 1/2. The dimension of the noise is approximately 1.41.

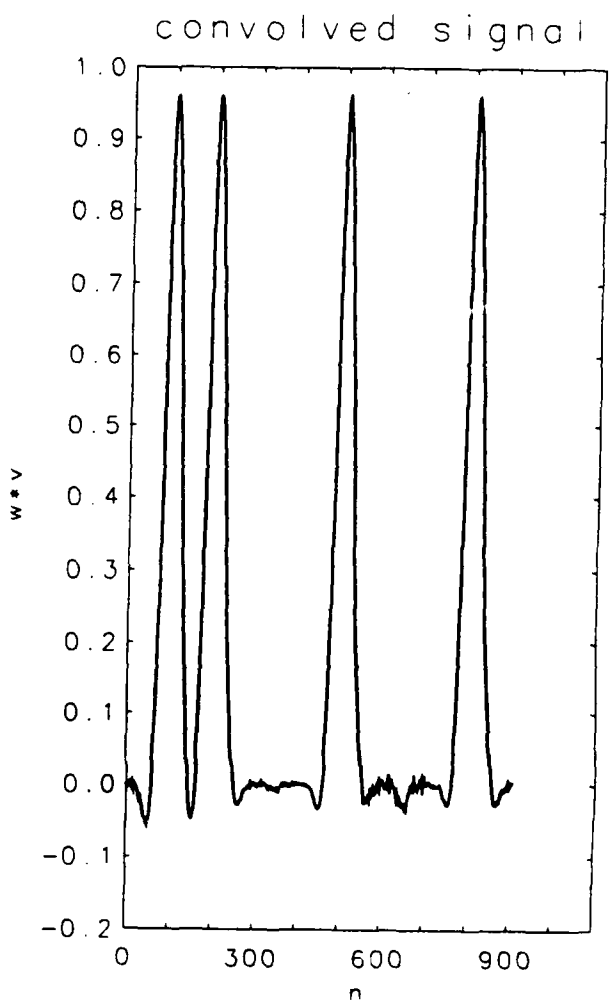

Fig. 10b — IFS-based convolution using a such that the noise dimension is approximately 1.4

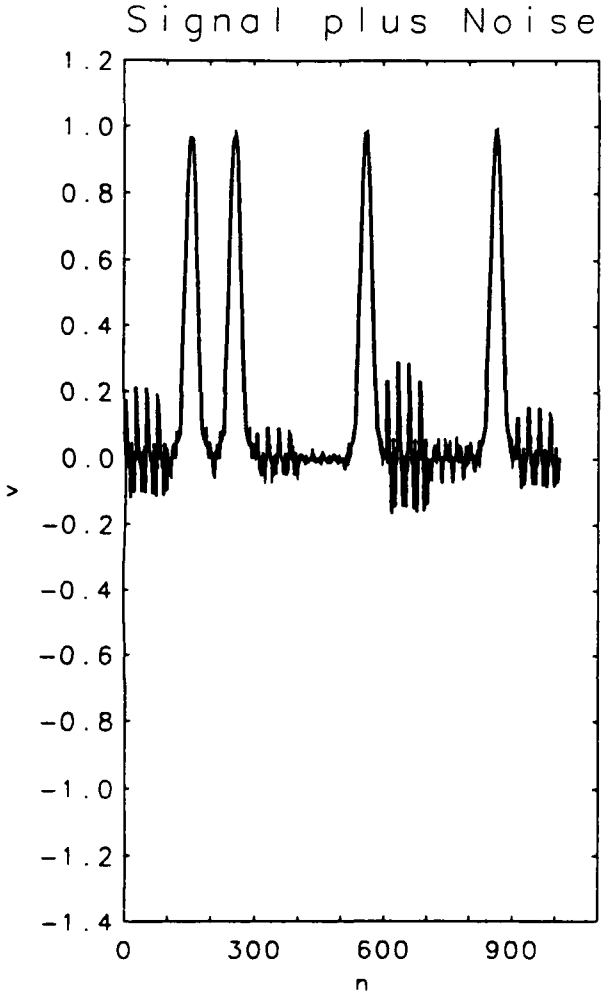

Fig. 10c — Same as in Fig. 10a

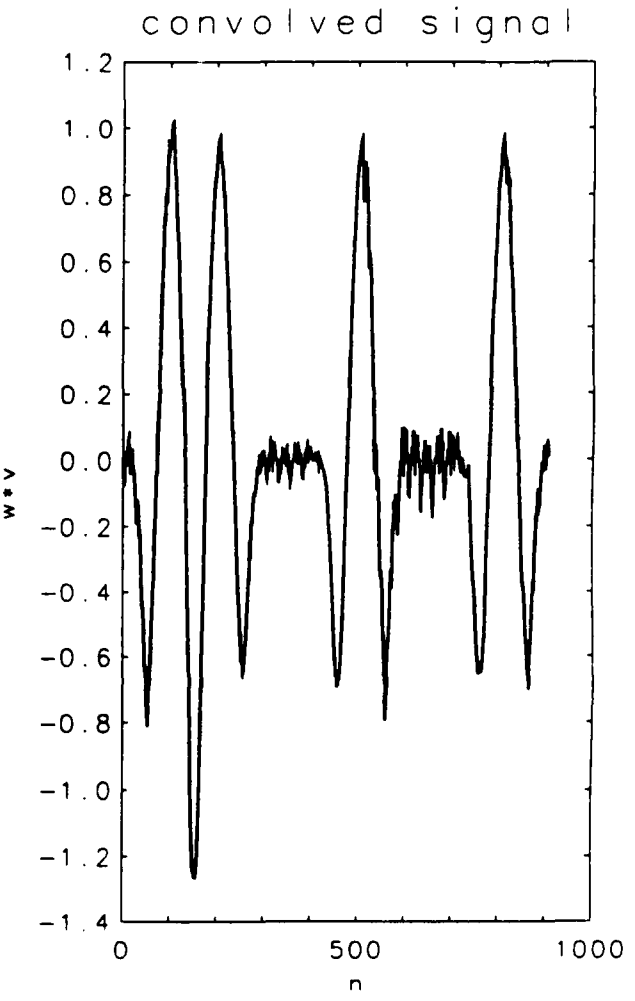

Fig. 10d — Same as in Fig. 10b, except the modelled noise has a dimension of 1.99

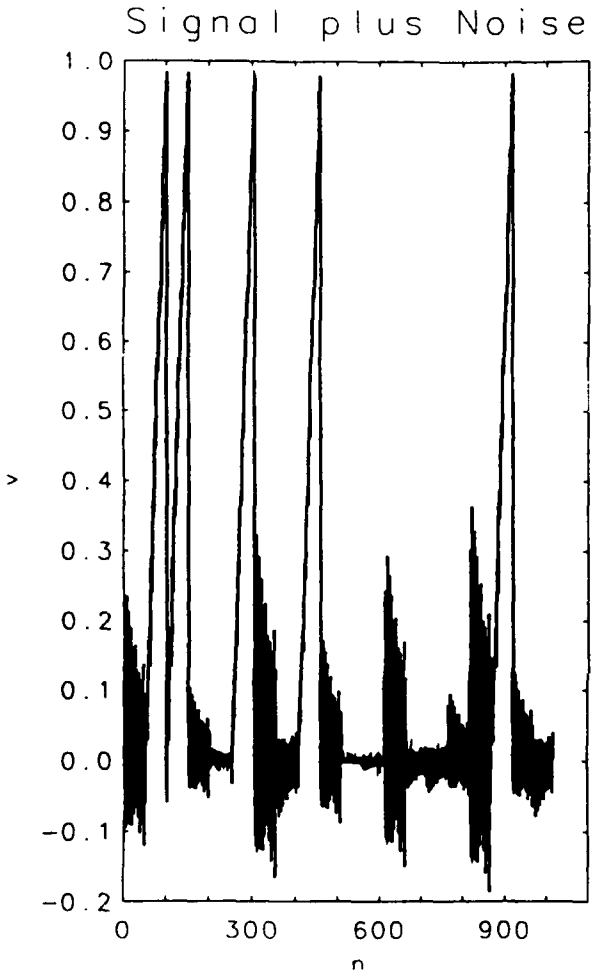

Fig. 11a — Signal plus noise, where the signal is a ramp, and the noise dimension is 1.41

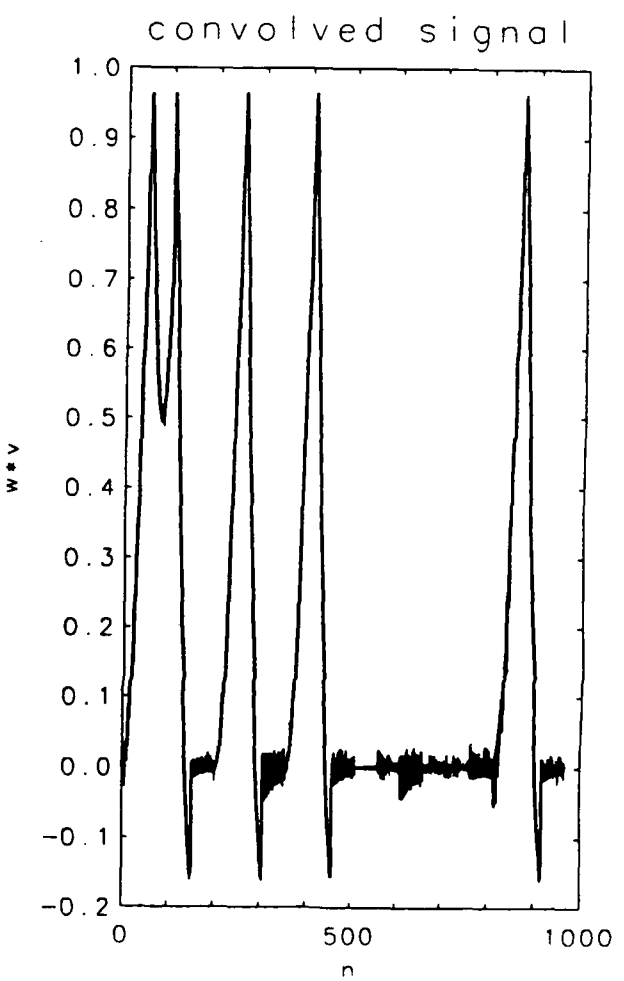

Fig. 11b — IFS-based convolution using a modelled noise having dimension 1.48

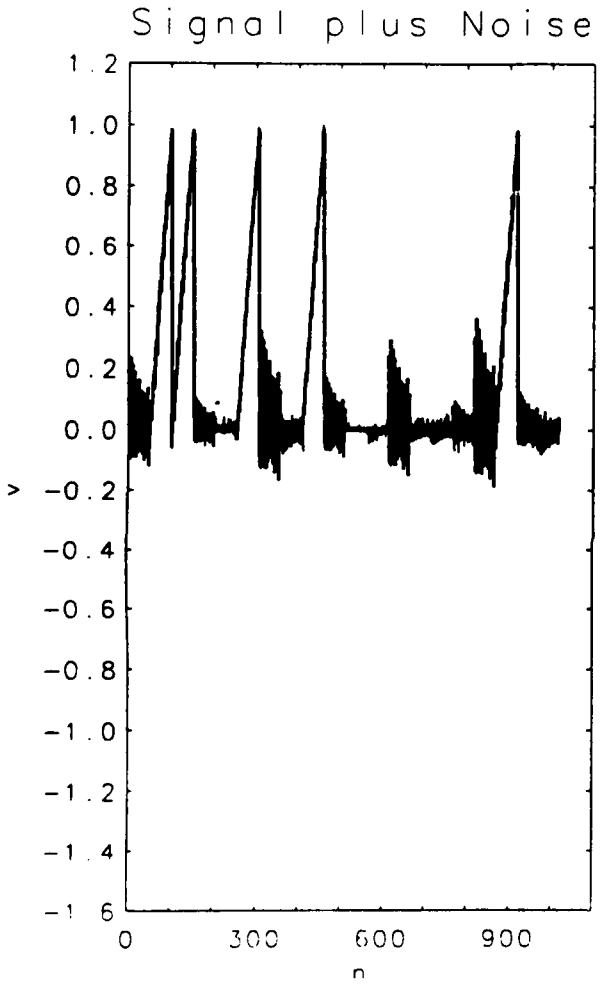

Fig. 11c — Same as in Fig. 11a

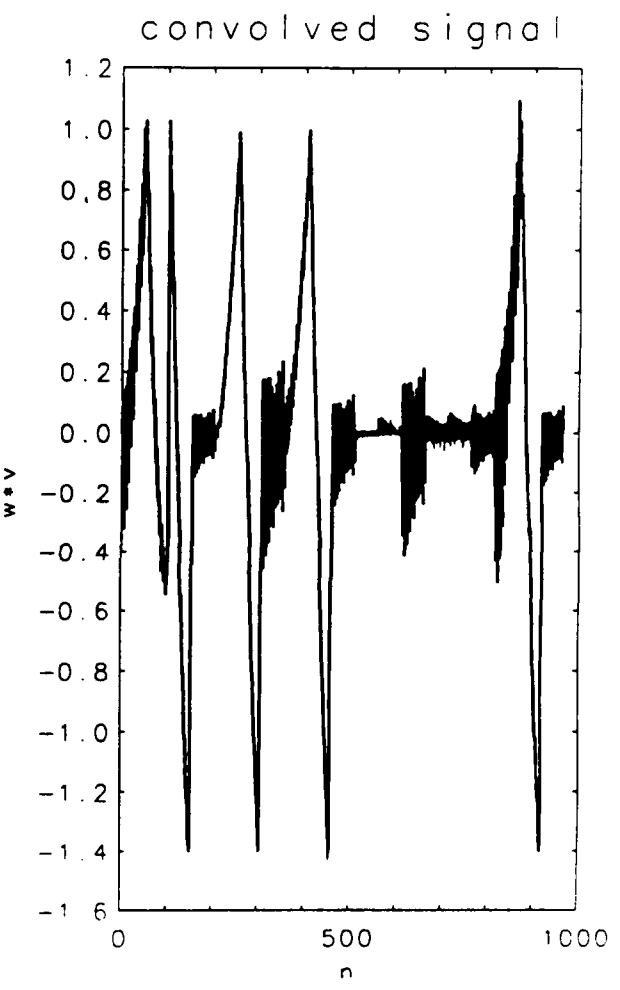

Fig. 11d — IFS-based convolution with modelled noise having dimension 1.97

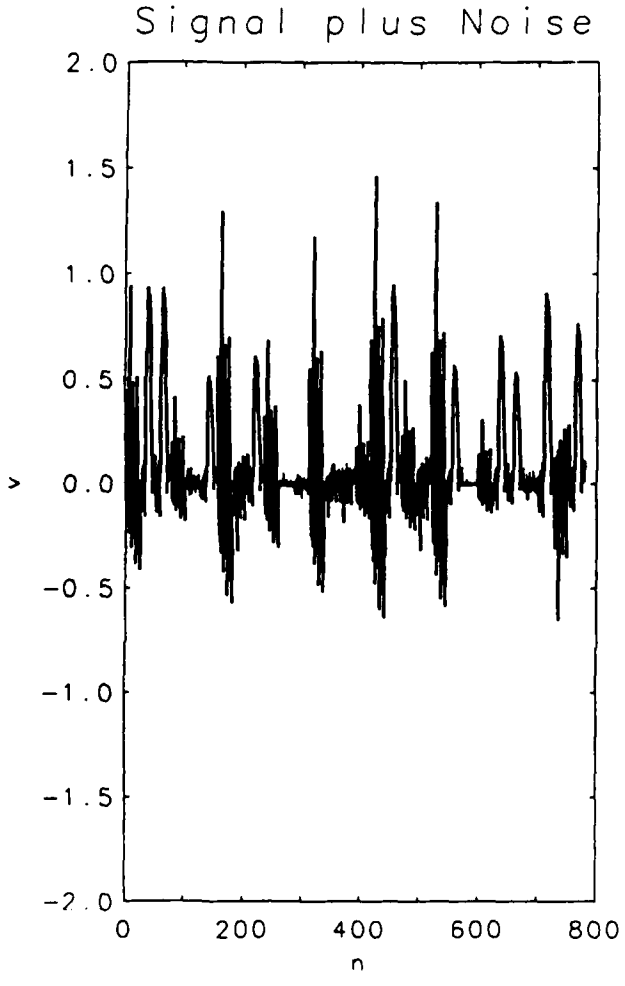

Fig. 12a — Signal plus fractal noise, The signal is normal with standard deviation of 1/2, and the background dimension is 1.41

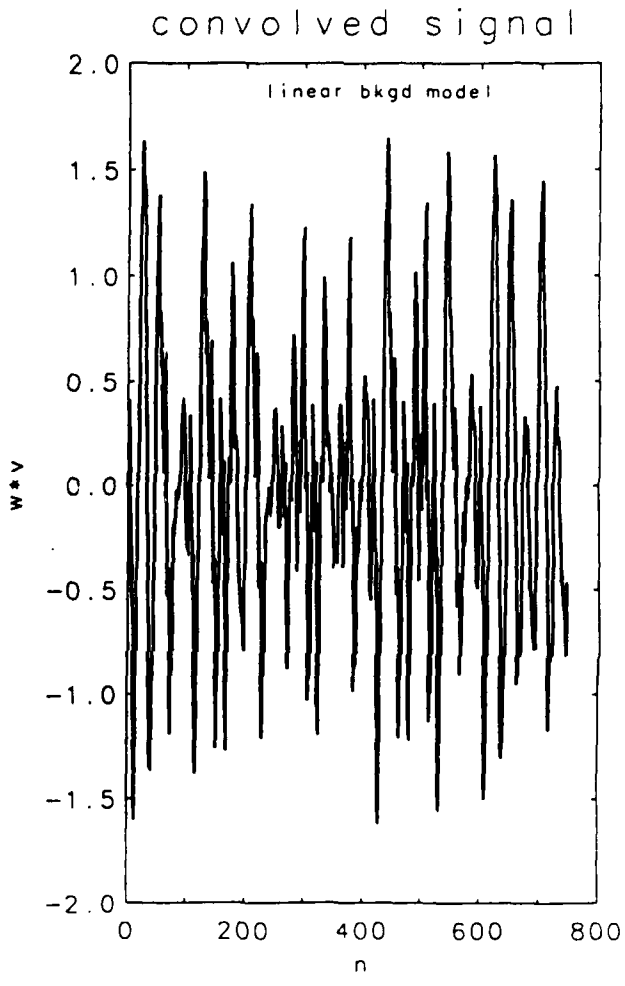

Fig. 12b — The convolved signal based on a filter derived using a linear background model. The filter is derived from the methods in Section 3 of the text.

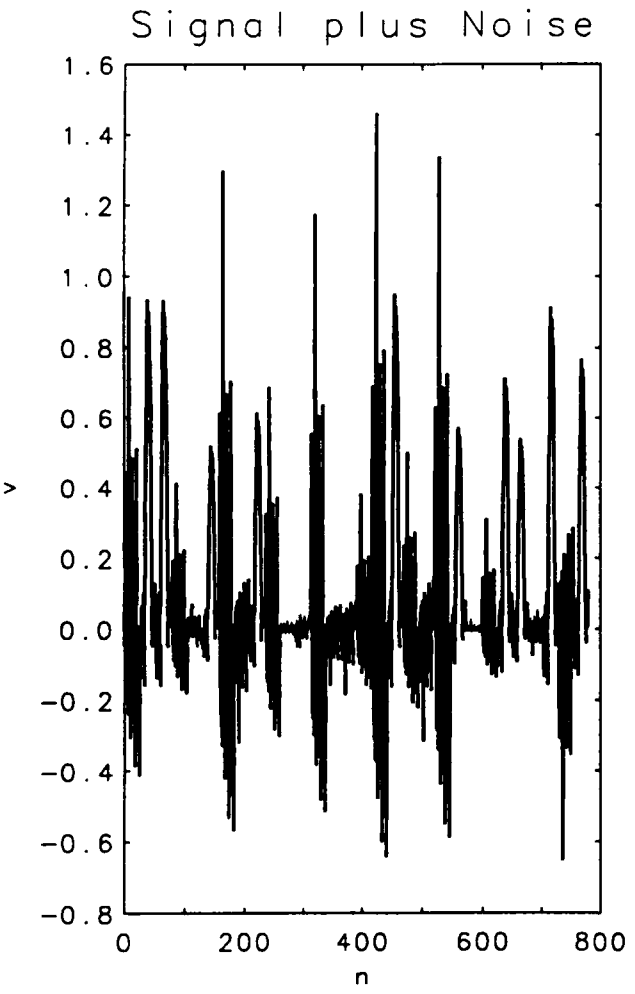

Fig. 12c — Same as Fig. 12a

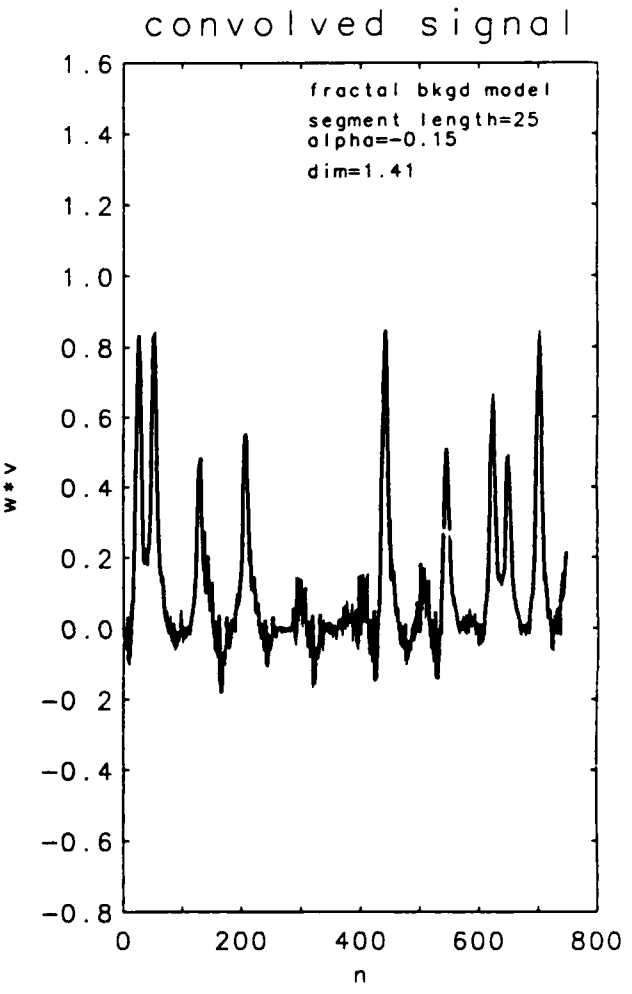

Fig. 12d — The convolved signal using a filter based on a fractal model of the background. The dimension of the modell background is equal to the simulated background.

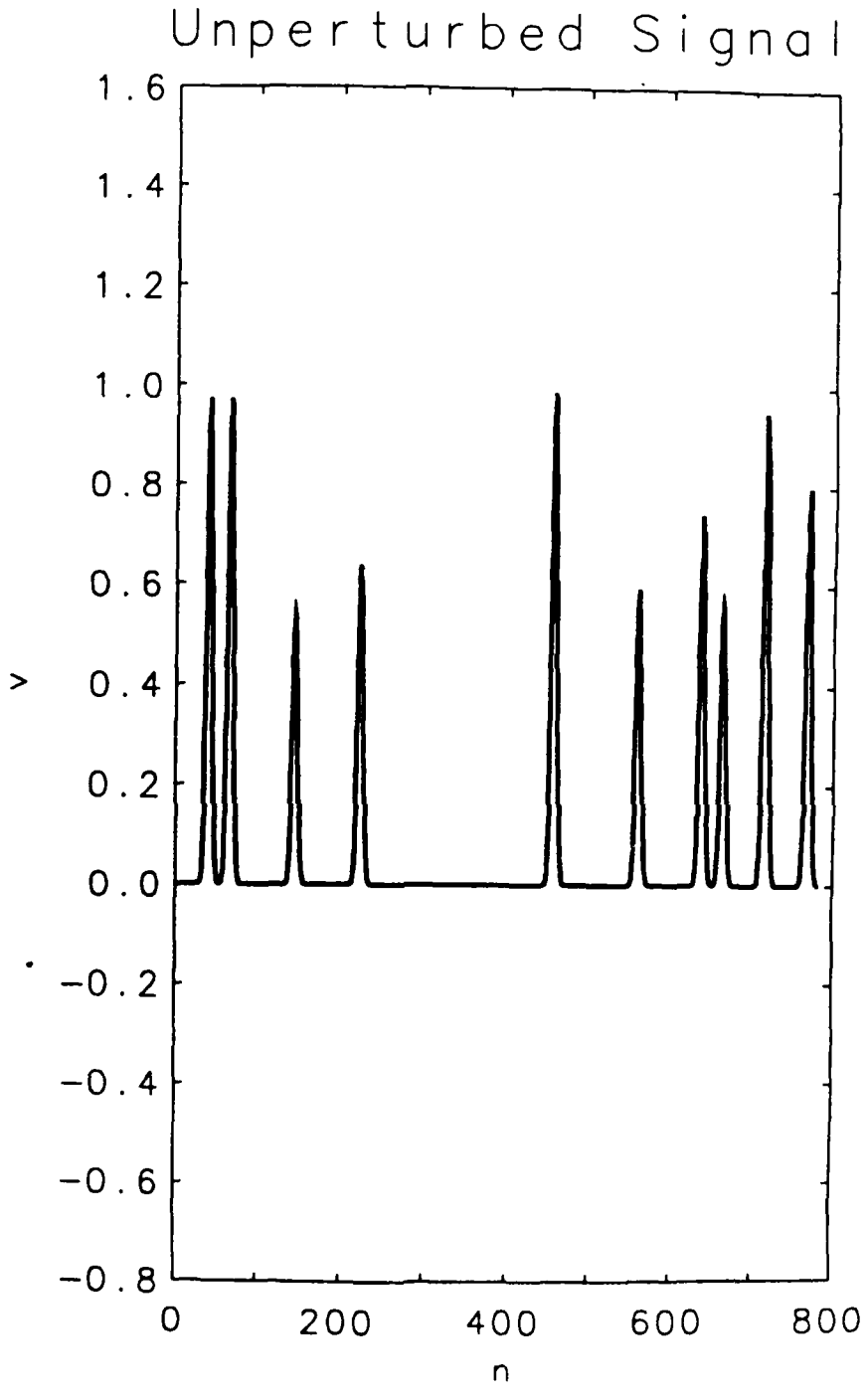

Fig. 12e — The original signal in the absence of noise. The signal is normal, and was used in Figs. 12a and 12c